Reply on “Climate impact on the development of Pre-Classic Maya civilization”

We thank the two reviewers for their constructive comments on our paper “Climate impact on the development of Pre-Classic Maya civilization”. We are happy to read that according to the reviewers our two palaeo-precipitation records add valuable new sources of palaeodata for the understanding of human environmental interaction in the Central Maya Lowlands (RC-1 and RC-2).

1. General commentary (RC-1)

Many of the main comments of RC-1 are related to the structure of the paper:

The structure of the paper after the methods is quite muddled and difficult to determine a consistent focus. Reorganization of this section with clearly defined results separated from discussion of those results may help.

I believe many of main points of your discussion are already present in this manuscript, but the structure at present does not bring these points to the forefront.

Finally, the abrupt ending of the paper left me feeling like this was an incomplete draft.

Make sure the ideas you highlight at the beginning of the paper (e.g., role of floods in Maya myth, the benefit of having the paired but different size watersheds of the beach ridges and lakes, etc.) are brought up again or emphasized throughout the paper.

We followed RC-1 recommendations and thoroughly restructured paragraph 3 and 4, and added a paragraph with conclusions which will hopefully meet RC-1 expectations.

3. Results

Beach-ridge record

Diatom record lake Tuspan

Wavelet transfer functions

4. Discussion

4.1 Climate change in the CML during the Pre-Classic period

Early Pre-Classic period (1800 – 1000 BCE)

Middle Pre-Classic period (1000 – 400 BCE)

Late Pre-Classic period (400 BCE – 250 CE)

4.2 Precipitation variability

Precipitation variability over long time scales

Centennial scale precipitation variability

4.3 Precipitation versus human development in the CML

5. Conclusions

5. Conclusions

For the first time a regional palaeo-precipitation record has been reconstructed for the Central Maya Lowland (CML), based on an exceptionally well dated high resolution beach ridge record. This record indicates centennial scale precipitation fluctuations during the Pre-Classic period that are not always registered in local records, adding valuable new insights into larger scale climatic forcing mechanisms for the CML. The generally poor correlation between the regional and local palaeo-precipitation reconstructions are probably related to spatial precipitation variability, and chronological uncertainties of many records. Additional research of beach ridge formation processes are needed to extend this regional precipitation reconstruction to the Classic and Post-Classic period.

We have also generated a local scale palaeo-precipitation record using diatoms preserved in a core from Lake Tuspan, thereby adding an alternative proxy to the relatively high number of local reconstructions predominantly based on oxygen isotope variability. We recognise, however, that diatom preservation is often poor in the carbonate lakes across the wider region. As a result, the correlation between these two reconstructions is variable through time.

Although the occurrence of a prolonged drought during the end of the Early Pre-Classic period, which we report here, is evident in other palaeo-precipitation reconstructions from the CML, the subsequent wet period during the Middle Pre-Classic period, registered in both our new records, is less evident elsewhere. Although many researchers have focused on the impact of drought on the development and disintegration of Maya societies, one should consider this prolonged wet period as potentially unfavourable for the development and intensification of agriculture in the CML, particularly in the wetter areas. We cannot be certain about the impact of wetter conditions on the Maya. However, owing to the lack of the development at this time we theorise that the wet period could have created poor growing conditions for maize in the CML. In order to test theory, we advocate for the use of process-based modelling approaches which capture heterogeneous environmental constraints on crop growth for given climate boundary conditions such as the approach applied by Dermody et al. (2014).

Our results provide evidence that North Atlantic atmospheric-oceanic forcing plays an important role in the modulation of the observed centennial scale precipitation variability, however further studies are required which compare well-dated terrestrial reconstructions that capture regional signals with solar and oceanic reconstructions to gain a better understanding of climate forcing mechanisms, both in the CML and across the wider region.

Dermody, B.J., van Beek, R.P.H., Meeks, E., Klein Goldewijk, K., Scheidel, W., van der Velde, Y., Bierkens, M.F.P., Wassen, M.J., Dekker, S.C., A virtual water network of the Roman world. Hydrol. Earth Syst. Sci. 18, 5025–5040, 2014.

2. Line by line commentary (RC-1)

71-72: The use of ’likely’ twice here reads a little awkward

We agree: the second ‘likely’ has been removed.

106-111: Can you rephrase this sentence? It is very long and full of multiple clauses.
We agree. Sentence is split into two sentences:

Although multiple factors determine the final elevation of the beach ridges, it has been shown that during the period 1775 ± 95 BCE to 30 ± 95 CE (at 1σ), roughly coinciding with the Pre-Classic period, beach ridge elevation has primarily been determined by the discharge of the Usumacinta river. Low elevation anomalies of the beach ridges occur in periods with increased river sediment discharge, which in turn is the product of high precipitation within the river catchment.

131: In the methods section, you talk about elemental analysis through X-ray fluorescence and how you use that to identify floods, but in the background on Lake Tuspan, you only discuss diatoms. I was left trying to figure out why you brought up the elemental analysis and whether it was just supporting diatom conclusions or if you were using it as an independent proxy. Perhaps a few sentences in the background clarifying all the techniques you use to make a paleo precip lake signal would help.

We agree. We will give a more thorough description of lake Tuspan's core lithology and XRF results in the Results section. Appendix figure A4 will therefore be moved to the main text. This will likely also accommodate RC-1 request for a more balanced presentation of both records **[much of the background (e.g., line 92) emphasizes the beach ridge record and treats the lake as secondary/supplemental data]**.

152: Missing an extra line spacing. Line spacing added.

167: In the background, you discuss the beach ridges before the lake study, but it's flipped in the methods.
Indeed, we corrected this, and in the discussion section we more consistently discuss the beach ridge record first, followed by the diatom record.

167: It would be nice to have a brief restatement (maybe in the background) on how these ridges were dated rather than having the reader look up cited literature.

We agree. We therefore added the following sentence to the text:

The age distance model is based on 35 AMS 14C dated terrestrial macro-remains (mainly leaf fragments isolated from organic debris layers), and 20 OSL dated sand samples (determined on small aliquots of quartz grains) (Nooren et al., 2017b).

223: There is decent evidence of regional drying at the close of the late Preclassic. Does your record support this? Or does it not extend far enough to be confident?

We found a pronounced dry interval during the early part of the Late Pre-Classic Period centred around 275 BCE, but a drought around the close of the late Pre-Classic Period (around 150 – 250 CE), often related to the Pre-Classic collapse, occurred just after the period covered by our beach ridge record (1775 ± 95 BCE to 30 ± 95 CE (at 1σ)).

233: Long term drying trend in what? Your data? Perhaps describe what you think is the long-term trend of your data, because up to this point it is not clear based on your previous discussion (185-230) that there is a drying trend (it seems quite variable).

We agree. We moved the sentence to the Result section (*Diatom record lake Tuspan*), and rewrote it as: After relatively high/positive PC-1 values during the Middle and Late Pre-Classic Period we observe a decreasing trend in PC-1 values during the following Classic Period, indicating a gradual increase in lake water salinity. Low PC-1 values between 800 – 950 CE are in accordance with many palaeorecords from the area (Fig. A2) indicating periods of prolonged droughts during the Late Classic Period.

233-239: This whole sections reads more like background information to set up your study rather than discussing your findings. It also feels a bit out of place to discuss broad long term variability AFTER you've covered the short term, period by period results.

We moved this section to paragraph 4.2 (Precipitation variability) of the discussion section. We think that our given explanation of the long term drying trend is more than background information, and should be presented here.

The Macal Chasm record shows broad similarities in the timing of long-period dry events with many of the other paleorecords in the region, although this is based on visual matching and not statistical work like wavelet analysis. Why do you think that the Macal Chasm record is the only one to show a match? Some discussion of whether you feel this is due to actual environmental differences or if it is data quality/characteristic driven would be nice here.

We only performed our wavelet analyses between the beach ridge record and all proxy records presented in Fig. A3. Therefore, we are not able to quantitatively compare the Macal Chasm record with other local records. The coherence between the beach ridge record and the Macal-Chasm record may be related to the fact that both records are relatively well dated (as stated in line 251).

The Macal Chasm chronology is not particularly precise, especially compared to other stalagmite records in the region like from Yok Balum. The uncertainties in the chronology run 200-400 years in many cases. Even if this doesn't adversely affect your conclusions, you may wish to address this and at the very least qualify how you decided that Macal Chasm is considered 'well-dated'.

We will add 'relatively', and describe the Macal Chasm chronology as relatively well-dated. Although chronological uncertainties of the Macal Chasm record during the Pre-Classic Period are generally in the order of 150 years (at 1 σ), this is better than most other palaeorecords for this time period. The Yok Balum record encompassed the Classic and Post-Classic period but hardly extend into the Pre-Classic.

269: Why would this period be different? If you are going to tell us that it isn't an analogue, you need to explain why this period is such an aberration.

Good question, we actually don't fully understand how climate forcing mechanisms during the Pre-Classic Period were different from today. We will add after line 271: Probably due a more northerly mean position of the ITCZ during the Pre-Classic period precipitation responded differently to solar forcing then today.

241-281: I feel that this section is one of your weaker parts of the paper. I do not see a convincing argument laid out that the North Atlantic is driving your variations, although I catch a glimpse of it. I would start this section laying out how your record relates with the North Atlantic and atmospheric data and build the argument of what is driving the changes you observe in your data.

We agree that that the centennial scale precipitation variability is likely driven by North Atlantic atmospheric-oceanic forcing forms an important finding of our research. However further research, and the input of climatologists are needed to understand the observed correlation and climate forcing mechanisms. We have added this to the conclusions.

284-305: I also feel that this section is underdeveloped. You are arguing that overly wet conditions may have delayed maize agriculture development, and I think this can be a valid hypothesis. However, you earlier pointed out that climate instability may be to blame for delayed maize (line 76). You also do not supply evidence for your 'overly wet' hypothesis in the form of maize physiology or ethnographic studies. If the region became wetter overall, some low lying areas would be too wet for agriculture, but wouldn't other regions that are presently too dry become potentially productive? Could it simply be a coincidence that local maize varieties hadn't been selected enough for local adaptation until the boom in agricultural clearance you note? Or that populations grew enough in the 'wet' years to support the increased social structures required for large scale agriculture and societal development, rather than maize being actively suppressed by the climate? These alternatives may not be valid, but I don't feel that your argument for wet = bad for maize = suppression of societal development makes enough of a causative case to defend itself against alternative theories. In particular, many have argued that the Classic Period was relatively wetter (e.g., YOK-1, Chicancanab) and this drove societal development and population growth. Others (e.g., Macal Chasm) argued that their data doesn't support a wetter Classic and that other factors, such as climate stability, are more important than wetter vs drier. Where does your research land on this issue? Overall, I think you need to discuss the Maya-environment interactions in much more depth if you wish to make arguments of a somewhat environmentally-deterministic nature.

We are glad that reviewer 1 considers our hypothesis that wet conditions may have delayed the development of maize agriculture a valid hypothesis. However his suggestion for a more in depth discussion of the agricultural and archaeological implications goes beyond the scope of this article, and will need further research, particularly from an archaeological point of view. At this stage we think it is important to point out that one should not only consider prolonged droughts as negative for the development of human societies in the area. We have added in the main text the following: We cannot be certain about the impact of wetter conditions on the Maya. However, owing to the lack of the development at this time we theorise that the wet period could have created poor growing conditions for maize in the CML. In order to test theory, we advocate for the use of process-based modelling approaches which capture heterogeneous environmental constraints on crop growth for given climate boundary conditions such as the approach applied by Dermody et al. (2014).

306: A very abrupt end without any concluding statements. I was left with, "Wait, what was the point or points they really wanted me to focus on?"

A paragraph with conclusions has been added to the text.

3. Line by line commentary (RC-2)

26 I'd change "while" to "whereas" as you are contrasting what the two records show

Agree.

28 I believe it is more conventional to use a little pyramid symbol for the delta 14C

Both are in use.

47 I suggest something like "Evidence for such impacts is found in the fact that floods, as well as droughts, are important themes:

Agree.

49 change "Mayan" to "Maya" (the former refers to the language(s))

Agree

58 Tankersley et al. also made the pitch that the "Maya clay" had a volcanic origin. But it is important to be clear about how that is meant.

Agree, we have added a reference to Tankersley et al. (2016) and changed sentence 58:

…., and past volcanic activity could have been responsible for the deposition of smectite rich clay layers in inland lakes (Tankersley et al., 2016; Nooren et al., 2017a).

Tankersley, K.B., Dunning, N.P., Scarborough, V., Huff, W.D., Lentz, D.L., and Carr, Catastrophic volcanism and its implication for agriculture in the Maya Lowlands: Journal of Archaeological Science 5, 465–470, 2016.

72 delete "likely" – it appears on line 71

Agree.

85-86 It may be that many of the differences among paleo-precipitation records reflect constraints on dating.

Indeed, few well-dated records exist for the Central Maya Lowlands.

108 change "has primarily been determined" to "was primarily determined" Done.

136 Maybe it is worth noting that this is not the Rio Dulce that drains Lake Izabal (eastern Guatemala) Done.

140 change to "exceeding a one-standard-deviation threshold" Done.

164 change "by" to "of" Done.

179 change "hematite stained" to "hematite-stained" 229 change "for" to "of" Done.

233 change "last thousands of years" to "last few thousand years" Done.

241 change "Centennial scale" to "Centennial-scale" Done.

245 You use "The in-phase relationship between the two records is significant above a 5% confidence level at centennial timescales during the Pre-Classic Period." As stated, I am not sure what that means. Do you really mean that you set the alpha value at 5%, and the probability of concluding the records are in-phase, when in fact they are not, is <5%. I think that should be re-worded for clarity.

We have added the following to section 2 (Methods): CWT applies Monte Carlo methods to test for significance. In this case we set the alpha value at 5%. Time periods and periodicities enclosed within the black lines of in our wavelet analysis indicate common power between timeseries with 95% confidence.

248 change to "at a centennial time scale" Done.

252 change to "gives us confidence" (refers back to "The coherence") Done.

254 and 257 I believe it is more conventional to use a little pyramid symbol for the delta 14C

Both are in use.

258 change to “¬500-year” Done.

266 change to “At that time” Done.

276 change to “centennial-scale” Done.

279 change “due to” to “as a consequence of” and later in the line to “because of” Done.

284 change to “During that period” Done.

290 change to “Between 1000 and 850 BCE” Done.

292 change “at” to “on” Done.

295 change to “for further development” Done.

301 change to “show strong and steady development” Done.

304-305 Again, I wonder if it is drier conditions, or perhaps as important, how the rainfall was distributed through the year. Agriculture is practiced across a large gradient of annual rainfall today, using traditional methods.

We agree. We added after sentence 305:

Changes in the distribution of rainfall probably also changed, and large floods, most evident during the Archaic and early Pre-Classic period, occurred much less frequently after approximately 1000 BCE.

623 change extend” to “extent” or “area” Done.

630 I did not know what was meant by “the Cariaco record is conform updated age-depth model.” Why not just say “We used an updated age-depth model for the Cariaco record.” Done.

632 and 637 I believe it is more conventional to use a little pyramid symbol for the delta 14C

Both are in use.

639 change to “500-yr” Done.

653 insert a period after “et al” Done.

653 change to “Long-term” Done.

668 Italicize “Aulacoseira” and “Pinus” (the latter in 3 places) Done.

671 change “Ti -15 point running mean” to “Ti 15-point running mean” Done.

675 change to “1-4-cm-thick” Done.

676 change to “light-coloured” Done.

685 change to “concentrations” Done.

687 change to “4-12-cm” Done.

690 change to “events” Done.

692 change to “linear” Done.

693 change to “radiocarbon-dated” Done.

704 change “at al.” to “et al.” Done.

711 change to “linear” Done.

711 change to “4th-order” Done.

Figure A1. How was it decided which archaeological sites to include? There are certainly many more, and this may mislead readers who are unfamiliar with the archaeology of the region. Also, might another colour be used for the Dulce River catchment. It appears that the area received >4000 mm/yr rainfall, being dark blue.

The colour of the Dulce river catchment has been adjusted, and in the figure legend ‘archaeological site’ has been changed to ‘major archaeological site’.

Figures 3, A2a, A2b. Is there any utility in indicating on those plots which way is drier and which is wetter? Also, for A2b, I suspect that the orange pollen percentages for Peten-Itza are “Montane” rather than “Montana”

We have added some arrows in Figure 3 to indicate if excursion indicate drier of wetter conditions.

We added to Figure caption A2: Notice that the y-axis is sometimes reversed, so that excursion above the x-axis always indicate relatively drier conditions.

Montane indeed !

Figure A10 – change to “linear” Done.

Climate impact on the development of Pre-Classic Maya civilization

Authors

Kees Nooren[1], Wim Z. Hoek[1], Brian J. Dermody[1~~,2~~], Didier Galop[3~~2~~], Sarah Metcalfe[4~~3~~], Gerald Islebe[5~~4~~] and Hans Middelkoop[1].

Affiliations

[1]Utrecht University, Faculty of Geosciences, 3508 TC Utrecht, The Netherlands;
[2]Utrecht University, Copernicus Institute of Sustainable Development, 3508 TC Utrecht, The Netherlands;

[3~~2~~]Université Jean Jaurès, CNRS, UMR 5602 GEODE, 31058 Toulouse, France;
[4~~3~~]University of Nottingham, School of Geography, Nottingham NG7 2RD, UK
[5~~4~~]El Colegio de la Frontera Sur, Unidad Chetumal Herbario, Chetumal, AP 424 Quintana Roo, Mexico;

Correspondence to: Kees Nooren (k.nooren@gmail.com)

Keywords

Pre-Classic Maya period, Central Maya Lowlands, climate record, beach ridges, palaeo-precipitation, 500-yr periodicity, 2.8 ka event.

Abstract

The impact of climate change on the development and disintegration of Maya civilization has long been debated. The lack of agreement among existing palaeoclimatic records from the region has prevented a detailed understanding of regional-scale climatic variability, its climatic forcing mechanisms, and its impact on the ancient Maya. We present two new palaeo-precipitation records for the Central Maya Lowlands, spanning the Pre-Classic period (1800 BCE – 250 CE), a key epoch in the development of Maya civilization. ~~Lake Tuspan's diatom record is indicative of precipitation changes at a local scale, whereas~~ile ~~A~~a beach ridge elevation record from world's largest late Holocene beach ridge plain provides a regional picture, while Lake Tuspan's diatom record is indicative of precipitation changes at a local scale. We identify centennial-scale variability in palaeo-precipitation that significantly correlates with the North Atlantic $\delta^{14}C$ atmospheric record, with a comparable periodicity of approximately 500 years, indicating an important role of North Atlantic atmospheric-oceanic forcing on precipitation in the Central Maya Lowlands. Our results show that t~~T~~he Early Pre-Classic period was characterized by relatively dry conditions, shifting to wetter conditions during the Middle Pre-Classic period, around the well-known 850 BCE (2.8 ka) event. We propose that this wet period may have been unfavorable for agricultural intensification in the Central Maya Lowlands, explaining the relatively delayed development of Maya civilization in this area. A return to relatively drier conditions during the Late Pre-Classic period coincides with rapid agricultural intensification in the region and the establishment of major cities.

1. Introduction

During the last decades, a wealth of new data has been gathered to understand human-environmental interaction and the role of climate change in the development and disintegration of societies in the Maya Lowlands (e.g., Akers et al., 2016; Douglas et al., 2015, 2016; Dunning et al., 2012, 2015; Lentz et al., 2014; Turner and Sabloff, 2012). Previous studies have emphasized the impact of prolonged droughts and their possible link with social downturn, such as the Pre-Classic Abandonment and the Classic Maya Collapse (Ebert et al., 2017; Hoggarth et al., 2016; Lentz et al., 2014; Kennett et al., 2012; Medina-Elizalde et al., 2010, 2016; Haug et al., 2003; Hodell et al., 1995, 2001, 2005~~; Haug et al., 2003~~). Less attention has been given to episodes of excessive rain and floods that may also have severely impacted ancient Maya societies (e.g. Iannone et al., 2014). Evidence for such impacts is found in~~This may be testified by~~ the fact that floods, as well as droughts, are an important theme depicted in the remaining ancient Maya codices (Fig. 1) (Thompson, 1972), and Maya~~n~~ mythological stories (Valásquez Garciá, 2006).

One of the main challenges in palaeoclimatic reconstructions is to unravel climate from human induced changes. Maya societies played a key role in the formation of the landscape, but the degree of human induced impact remains highly debated (Hansen, 2017; Beach et al., 2015; Ford and Nigh, 2015). For example, it is proposed that the increase in sedimentation rate after 1000 BCE at Lake Salpeten (Anselmetti et al., 2007) and Peten-Itza (Mueller et al., 2009) is related to human induced soil erosion.

However, other high resolution lake records from the area do not show a significant increase in sedimentation rate during the Pre-Classic or Classic period (e.g. Wahl et al., 2014), and past volcanic activity could have been responsible for the deposition of smectite rich clay layers in inland lakes ~~'Maya Clay'~~ (Tankersley et al., 2016; Nooren et al., 2017a). Palynological records from the Central Maya Lowlands (CML, Fig. 2) show no evidence of widespread land clearance and agriculture before ~400 BCE (Wahl et al., 2007; Islebe et al., 1996; Leyden et al., 1987), and there is growing consensus that the decline in the percentage of lowland tropical forest pollen during the Pre-Classic period (Galop et al., 2004;~~;~~ Islebe et al., 1996; Leyden et al, 1987) was caused by climatic drying instead of deforestation (Torrescano and Islebe, 2015; Wahl et al., 2014; Mueller et al., 2009).

In this paper, we present two new palaeo-precipitation records reflecting precipitation changes in the CML. The records span the Pre-Classic period (1800 BCE – 250 CE), when Maya societies in the CML transformed from predominantly mobile hunter-gatherers in the Early Pre-Classic p~~P~~eriod (e.g. Inomata et al., 2015; Coe, 2011; Lohse, 2010), to complex sedentary societies that founded impressive cities like El Mirador by the later part of the Pre-Classic period (Hansen, 2017; Inomata and Henderson, 2016). The period of rapid growth in these centralized societies probably~~likely~~ occurred much later than previously thought, ~~likely~~ sometime after the start of the Late Pre-Classic period around 400 BCE (Inomata and Henderson, 2016). This raises the question for the reason behind the delayed development of societies in this area, which was to become the core area of Maya civilization during the following Classic period (250 – 900 CE). There is recent evidence that climate during the Middle Pre-Classic Period (1000 – 400 BCE) may have been less stable than recently reported (Ebert et al., 2017). We ~~hypothesize~~ propose that anomalously wet conditions ~~that climate during the Middle Pre-Classic Period (1000 – 400 BCE) may have been less stable than recently reported (Ebert et al., 2017), and~~ could have been unfavourable for the intensification of maize-based agriculture, which formed the underlying subsistence economy responsible for the development of many neighbouring Mesoamerican societies during this period.

The CML have been intensively studied, and several well-dated speleothem, palynological, and limnological records have been obtained for this area (Díaz et al., 2017; Akers et al., 2016; Douglas et al.; 2015; Wahl et al., 2014; Kennett et al., 2012; Mueller et al., 2009; Metcalfe et al., 2009; Domínguez-Vázquez and Islebe, 2008; Galop et al., 2004; Rosenmeier et al., 2002; Islebe et al., 1996) (Fig. 2 and A1). However, palaeo-precipitation signals from these records and those from adjacent areas in the Yucatan and Central Mexico exhibit large differences among records (Fig. A2), making the reconstruction and interpretation of larger-scale precipitation for the region a challenge (Lachniet et al., 2013, 2017; Douglas et al., 2016; Metcalfe et al., 2015). Existing climate reconstructions mostly represent local changes and are predominantly based on oxygen isotope variability, although some new proxies have been introduced recently (e.g. Díaz et al., 2017; Douglas et al., 2015).

We present a regional-scale palaeo-precipitation record for the CML, extracted from world's largest late Holocene beach ridge sequence at the Gulf of Mexico coast (Fig. 2B). The beach ridge record captures changes in river discharge resulting from precipitation patterns over the entire catchment of the Usumacinta River and thus represents regional changes in precipitation over the CML (Nooren et al., 2017b). Currently the annual discharge of the Usumacinta river is approximately 2000 m^3/s, corresponding to ~40 % of the excess or effective rain falling in the 70,700 km^2 large catchment (Nooren et al., 2017b). Mean annual precipitation within the catchment is ~2150 mm, with 80 % falling during the boreal summer, related to the North American or Mesoamerican Monsoon system (Lachniet et al., 2013, 2017; Metcalfe et al., 2015). The interpretation of the beach ridge record is supported by a new multi-proxy record from Lake Tuspan, an oligosaline lake situated within the CML. The lake r~~,~~ ~~r~~eceives~~ing~~ most of its water from a relatively small catchment of 770 km^2 (Fig. 2) and hence provides a local precipitation record, to complement the regional signal from the beach ridge sequence.

Regional palaeo-precipitation signal

The coastal beach ridges consist of sandy material originating from the Grijalva and Usumacinta rivers, topped by wind-blown beach sand (Nooren et al., 2017b). Although multiple factors determine the final elevation of the beach ridges, it has been shown that during the period 1775 ± 95 BCE to 30 ± 95 CE (at 1σ), roughly coinciding with the Pre-Classic period, beach ridge elevation w~~h~~as primarily ~~been~~ determined by the discharge of the Usumacinta river.~~,~~ L~~in a counter-intuitive manner: l~~ow elevation anomalies of the beach ridges occur in periods with increased river sediment discharge, which in turn is the product of high precipitation within the river catchment. Under these conditions, beach ridges develop relatively rapidly, and are exposed to wind for a shorter period. In contrast, during periods of drought, sediment supply to the coast is reduced, resulting in a decreased seaward progradation rate of the beach ridge plain. This leaves a longer period for aeolian accretion on the beach ridges near the former shoreline, resulting in higher beach ridges (Nooren et al., 2017b). Hence, variations in beach ridge elevation reflect changes in rainfall over the Usumacinta catchment, and thereby represent catchment-aggregated precipitation, rather than~~instead~~ ~~of~~ a local signal. The very high progradation rates and the very robust age-distance model (Fig. A3), with uncertainties of the calibrated ages not exceeding 60–70 years (at 1σ), effectively allow the reconstruction of palaeo-precipitation at centennial time scales.

Local palaeo-precipitation signal: Lake Tuspan record

~~Diatom communities within oligo- to hypersaline lakes are strongly influenced by lake water salinity (Reed, 1998; Gasse et al., 1995), and we therefore determined diatom assemblage changes within the Lake Tuspan sediment record (Fig. 3) to reconstruct palaeo-salinities of the lake water, reflecting palaeo-precipitation in the lake's catchment.~~ During dry periods, a reduced riverine input of fresh water and a lowering of the lake level enhance the effect of evaporation and increase the salinity of the lake water. Diatom communities within oligo- to hypersaline lakes are strongly influenced by lake water salinity (Reed, 1998; Gasse et al., 1995), and we therefore determined diatom assemblage changes within the Lake Tuspan sediment record (Fig. 3) to reconstruct palaeo-salinities of the lake water, reflecting palaeo-precipitation in the lake's catchment via changes in the balance of precipitation - evaporation. ~~The first principal component (PC-1) of the variability in the diatom assemblages is interpreted as an indicator of lake water salinity (Fig. 3). This interpretation is supported by the fact that high PC-1 values are accompanied by relatively high percentages of *Plagiotropis arizonica* (Fig. A4), a diatom species characteristic of high-conductivity water bodies (Czarnecki and Blinn, 1978).~~

2. Methods

Beach ridge sequence

Beach ridges elevations were extracted from a Digital Elevation Model (DEM) of the coastal plain along the transects indicated in Fig. 2 (Nooren et al., 2017b). The DEM is based on LiDAR data originally acquired in April-May 2008 and processed by Mexico's National Institute of Statistics and Geography (INEGI), Mexico. The relative beach ridge elevation is defined as the difference between the beach ridge elevation and the long-term (~500 yr) running mean (Fig. A3). The age distance model is based on 35 AMS ^{14}C dated terrestrial macro-remains (mainly leaf fragments isolated from organic debris layers), and 20 OSL dated sand samples (determined on small aliquots of quartz grains)~~Details of the development of the age model for the beach ridges are given in~~ (Nooren et al., ~~(~~2017b).

Lake Tuspan

Two parallel cores, Tuspa~~á~~n cores B and C, were taken with a Russian corer (type GYK) in shallow water near the inflow of the Rio Dulce (not to be confused with the Rio Dulce that drains lake Izabal in eastern Guatemala), not far from core A which has been studied for pollen (Galop et al., 2004). Semi-quantitative analyses of Si, S, K, Ca, Ti, Mn and Fe were conducted on both cores with an X-ray fluorescence core scanner (type AVAATECH) at 0.5 cm intervals. Deposits of large floods were identified on the basis of elevated concentrations of Si, Fe, Ti and Al (Davies et al., 2015), with peak concentrations exceeding an~~t least the~~ one~~-~~standard~~-~~deviation threshold above the mean.

Core C was investigated for amorphous silica, charred plant fragments, and diatoms (Fig. 3, A4 and A5~~5~~). The core was subsampled at 4-12 cm contiguous intervals, each interval representing 25-80 years. In addition, 37 1-cm samples (representing ~6.5 yr) were processed using the method outlined by Battarbee (1973) to determine diatom concentrations and ~~to determine~~ short term~~ime~~ variability (decadal scale). Subsamples were treated with HCl (10 %) to remove calcium carbonate. Large organic particles were removed by wet sieving (250 µm mesh), and charred plant fragments > 250 µm were counted under a dissection microscope. Remaining organic material was removed by heavy liquid separation using a sodiumpolywolframate solution with a density of 2.0 g/cm^3. A silicious residue, denoted 'amorphous silica' was subsequently removed by heavy liquid separation using a sodiumpolywolframate solution with a density of 2.3 g/cm^3, and dry weight was determined after drying of the samples at 105°C.

Slides were prepared from the remaining material. Diatoms were identified, counted and reported as percentages of the total diatom sum, excluding the small and often dominant *Denticula elegans* and

Nitzschia amphibia species. These species show a large variability on short time scales (Fig. A5~~6~~), and are not indicative for changes at centennial time scale. We relate changes in diatom assemblages mainly to lake water salinity changes. The first principal component on the entire assemblage (PC-1) is interpreted as a palaeosalinity indicator. Diatom taxonomy is mainly after Patrick and Reimer (1966; 1975) and Novelo, Tavera, and Ibarra (2007). We identified *Plagiotropis arizonica* following Czarnecki and Blinn (1978), ~~and~~ *Mastogloia calcarea* following Lee et al. (2014), and *Cyclotella petenensis* following Paillès et al. (2018).

The age-depth model for core C is based on seven AMS radiocarbon dated terrestrial samples and stratigraphical correlation with core A (Fleury et al., 2014). We used a linear regression between the available radiocarbon dated samples (Fig. A7) which is comparable with the age-depth model of~~by~~ Fleury et al. (2014) for the time window between ~2500 BCE and 1000 CE.

~~*Beach ridge sequence*~~

~~Beach ridges elevations were extracted from a Digital Elevation Model (DEM) of the coastal plain along the transects indicated in Fig. 2 (Nooren et al., 2017b). The DEM is based on LiDAR data originally acquired in April-May 2008 and processed by Mexico's National Institute of Statistics and Geography (INEGI), Mexico. The relative beach ridge elevation is defined as the difference between the beach ridge elevation and the long-term (~500 yr) running mean (Fig. A3).~~

Wavelet transfer functions

The relation between our beach ridge and diatom record and other palaeo-precipitation records from the Maya Lowlands and nearby regions (figure A1 and A2) were investigated by wavelet coherence (CWT) analyses using the software developed by Grinsted et al. (2004). We also applied CWT to compare our record with North Atlantic ice drift record (Bond et al., 2001) and the Northern Hemispheric atmospheric $\delta^{14}C$ record (Reimer et al., 2013) to gain an understanding of the forcing of the regional changes in precipitation we observe. The record of drift ice from the North Atlantic ~~(Bond et al., 2001)~~ is bimodally distributed, oscillating between periods of low and high concentrations of hematite~~-~~stained grains. The timeseries was therefore transformed into a record of percentiles based on its cumulative distribution function to avoid leakage of the square wave into frequency bands outside the fundamental period (Grinsted et al., 2004). CWT applies Monte Carlo methods to test for significance. In this case we set the alpha value at 5%. Time periods and periodicities enclosed within the black lines of in our wavelet analysis indicate common power between timeseries with 95% confidence.

3. Results

Beach-ridge record

As described above, when beach ridge elevation is largely driven by the discharge of the Usumacinta River, ~~Between 1775 ± 95 BCE and 30 ± 95 CE (roughly coinciding with the Pre-Classic period), when beach ridge elevation was primarily determined by the discharge of the Usumacinta River (Nooren et al., 2017b),~~ periods of relative high (low) beach ridges correspond to relatively drier (wetter) conditions in the ~~catchment of the~~ Usumacinta catchment~~River~~ (Fig. 2). The beach-ridge record shows clear centennial scale variability, with an exceptionally dry phase cent~~e~~red around 1000 ± 95 BCE, and a subsequent pronounced wet phase cent~~e~~red around 800 ± 95 BCE.

Diatom record L~~l~~ake Tuspan

The sediment stratigraphy of core C can be divided into two main units. ~~Sediments from 0.25 to 4.3 m depth are vaguely laminated, with three distinct dm-thick turbidite layers (Fig. 3).~~ Below 4.3 m the core is clearly laminated, and 0.5-4-cm-thick dark palaeoflood-layers contrast with the predominantly light-coloured calcareous deposits. The flood-layers are characterized by elevated detrital input, resulting in elevated concentrations of Si~~ (cps = counts per second)~~, amorphous silica~~ca (% of dry weight)~~, and charred plant fragments~~ (number of particles/g dw)~~. The average recurrence time of large floods was approximately 50 years. Sediments from 0.25 to 4.3 m depth are vaguely laminated, with three distinct dm-thick turbidite layers (Fig. 3).

~~The first Principal Component axis (PC-1) of the diatom record is interpreted as a lake water salinity indicator, with low values corresponding to high salinity waters, reflecting relatively dry conditions (Fig. 3).~~ The~~is~~ interpretation of PC-1 (Fig. 3) as an indicator of lake salinity and hence relative dryness (see Methods) is supported by the fact that low/negative~~high~~ PC-1 values are driven~~accompanied~~ by relatively high percentages of *Plagiotropis arizonica* (Fig. 3), a diatom species characteristic of high-conductivity water bodies (Czarnecki and Blinn, 1978) as well as other benthic, high salinity/alkalinity species such as *Anomoeoneis sphaerophora* and *Craticula cuspidata* (~~see~~ Fig. A4).

A drastic change from dry to wet conditions occurred around 4.3 m depth (~1100 BCE), with the loss of salinity tolerant taxa and higher proportions of freshwater taxa such as *Eunotia* sp. -and *Cyclotella petenensis* ~~species~~ (Fig. 3). This ~~and~~ coincides with the observed lithological shift from clearly to vaguely laminated sediments. ~~.~~After relatively ~~The~~ high/positive PC-1 values~~diatom record then indicates~~ during the Middle and Late Pre-Classic Perioda we observe a decreasing trend in PC-1 values during the following Classic Period, indicating a ~~subsequent~~ gradual increase in lake water salinity ~~between 1000 BC and 950 CE~~. Low PC-1 values between 800 – 950 CE are in accordance with many palaeorecords from the area (Fig. A2) indicating periods of prolonged droughts during the Llate Classic Period.

Wavelet transfer function

Wavelet coherence (WTC) analysis (Grinsted et al., 2004) indicates in-phase coherence between the beach ridge record and the recently extended and revised calcite $\delta^{18}O$ speleothem record from Macal-Chasm cave (Akers et al., 2016) (Fig. A7~~8~~). The in-phase relationship between the two records is significant above a 5% confidence level at centennial timescales during the Pre-Classic Period. -We did not find significant relationships between the beach ridge record and other palaeo-precipitation records from the CML, nor with records from the Yucatan and Central Mexico (Fig. A2), except for a significant in-phase coherence at a centennial time scale with the *Pyrgophorus* sp. $\delta^{18}O$ record from Lake Chichancanab (Hodell et al., 1995).

4. Discussion

4~~3~~.1 Climate change in the CML during the Pre-Classic period

Early Pre-Classic pPeriod (1800 – 1000 BCE)

~~The Lake Tuspan diatom record (Fig. 3) indicates relatively dry conditions, comparable to those during the preceding Late Archaic Period (~5000 – 1800 BCE). Despite the predominantly dry conditions, large floods still occurred, as demonstrated by the repetitive input of fluvial material into the lake. These flood events are identifiable as distinctive dark layers of detrital sediment within the calcareous lake deposits, and are characterized by elevated concentrations of amorphous silica and charred plant fragments (Fig. 3 and A4). The average recurrence time of large floods was approximately 50 years, and periods with highest fluvial sediment input in Lake Tuspan coincided with periods of increased input of charcoal into Lake Peten-Itza (Schüpbach et al., 2015) (Fig. A2). Because the CML were still sparsely populated during the Early Pre-Classic period (Inomata et al., 2015) we relate the presence of charcoal to the occurrence of wildfires.~~

Both~~The~~ beach ridge and diatom records indicate that the onset of the early Pre-Classic pPeriod was relatively dry (Fig. 4).~~, comparable with the preceding Late Archaic Period (~5000 – 1800 BCE).~~ Despite the predominantly dry conditions, large floods still occurred, as demonstrated by the repetitive input of fluvial material into Llake Tuspan. Periods with the highest fluvial sediment input coincided with periods of increased input of charcoal into Lake Peten-Itza (Schüpbach et al., 2015) (Fig. A2). Because the CML were still sparsely populated during the Early Pre-Classic period (Inomata et al., 2015) we relate the presence of charcoal to the occurrence of wildfires.

After a transition to wetter conditions between 1500 and 1400 BCE, we observe ~~ch ridge record indicates~~ a drying trend that culminated in a prolonged dry period at the end of the Early Pre-Classic period centered around 1000 ± 95 BCE. Although this exceptionally dry phase is less apparent from Lake Tuspan's diatom record (Fig. 3), it has been recorded at many other sites within the CML. At Lake Puerto Arturo, high $\delta^{18}O$ values ion the gastropod *Pyrgophorus* sp. indicate that this was the driest period since 6300 BCE (Wahl et al., 2014), and the recently extended and improved speleothem $\delta^{18}O$ record from Macal Chasm indicates that this dry period was probably at least as severe as any prolonged droughts during the Classic and Post-Classic pPeriod (Akers et al., 2016). Dry conditions are reflected in high Ca/Σ(Ti,Fe,Al) values at Lake Peten-Itza (Mueller et al., 2009), indicating elevated authigenic carbonate ($CaCO_3$) precipitation relative to the input of fluvial detrital elements (Ti, Fe and

Al) during this period; w~~, and w~~ater level at this large lake must have dropped by at least 7 m (Mueller et al., 2009).

Middle Pre-Classic period (1000 – 400 BCE)

Both the beach ridge and the Lake Tuspan diatom records indicate a change to wetter conditions around 1000-850 BCE, causing major changes in hydrological conditions in the CML (Fig. 4~~3~~). The diatom assemblages in the Lake Tuspan record show a major change in composition. Species indicative of meso- to polysaline water almost completely disappear, and are replaced by species indicating fresh water conditions (Fig. ~~3 (PC1) and A~~4). In the lake sediments, this transition is also marked by a lithological shift from clearly to vaguely laminated ~~to more homogeneous~~ sediments that lack repetitive large flood layers, while charred plant fragments are almost absent until ~400 BCE. Similar abrupt lithological transitions were reported from Lake Chichancanab (Hodell et al., 1995) and Lake Peten-Itza (Mueller et al., 2009), and Wahl et al. (2014) describe a regime shift at Puerto Arturo. The sudden reduction in charred plant fragments around ~1000 BCE at Lake Tuspan coincides with reduced concentrations of charcoal at Lake Peten-Itza (Fig. A2) (Schupbach et al., 2015) and Laguna Tortuguero, Puerto Rico (Burney and Pigott Burney, 1994) indicating rapid climatic changes over a large spatial scale.

Late Pre-Classic period (400 BCE – 250 CE)

~~The diatom record at Lake Tuspan (Fig. 3) shows a general increase in lake water salinity, indicating a gradual shift to drier conditions in the Late Pre-Classic Period.~~ Both~~The~~ beach ridge and diatom record (Fig. 4~~3~~) indicate~~s~~ that a relatively dry period occurred by the onset of the Late Pre-Classic period, which has not been identified in other proxy records from the region (Fig. A2), although high *Pinus* pollen percentages in the pollen record from Petapilla pond near Copan (McNeil, 2010) during this period may indicate dry conditions, as high *Pinus* pollen percentage at highland sites could be indicative of~~or~~ drier conditions (Domínguez-Vázquez and Islebe, 2008). The diatom record at Lake Tuspan (Fig. 3) shows a general increase in lake water salinity, indicating a gradual shift to drier conditions in the Late Pre-Classic p~~P~~eriod.

4.2 Precipitation variability

Precipitation variability over long time scales

The observed general drying trend over the last few thousand~~s of~~ years is probably~~may be~~ related to the southward shift of the ITCZ during the late Holocene. The shift occurred in response to orbitally-forced changes in insolation (Haug et al., 2001), causing a gradual Northern Hemisphere cooling versus Southern Hemisphere warming (Fig. 4~~3~~), thereby shifting the ITCZ towards the warming southern hemisphere (Schneider et al., 2014). Wetter conditions during the Middle Pre-Classic period may reflect a~~A~~ more northerly position of the ITCZ, which ~~during the Pre-Classic period~~ may be related to stronger easterly tradewinds and the less frequent occurrence of winter season cold fronts~~during the Pre-Classic period~~, as beach ridge morphological changes suggest (Nooren et al., 2017b).

Centennial~~-~~scale precipitation variability

~~Wavelet coherence (WTC) analysis (Grinsted et al., 2004) indicates in-phase coherence between the beach ridge record and the recently extended and revised calcite $\delta^{18}O$ speleothem record from Macal-Chasm cave (Akers et al., 2016) (Fig. A8). The in-phase relationship between the two records is significant above a 5% confidence level at centennial timescales during the Pre-Classic Period. We did not find significant relationships between the beach ridge record and other palaeo-precipitation records from the CML, nor with records from the Yucatan and Central Mexico (Fig. A2), except for a significant in-phase coherence at centennial time scale with the *Pyrgophorus* sp. $\delta^{18}O$ record from Lake Chichancanab (Hodell et al., 1995).~~

The coherence between the beach ridge record and the relatively well-dated Macal-Chasm speleothem record gives us confidence that these records reflect regionally coherent variability at centennial timescales during the Pre-Classic period. Interestingly, the beach ridge record is significantly in anti-phase with the North Atlantic ice drift record (Bond et al., 2001) and the Northern Hemispheric atmospheric $\delta^{14}C$ record during the Pre-Classic Period (Reimer et al., 2013) (Fig. 5~~4~~), suggesting an important role of North Atlantic atmospheric-oceanic forcing on precipitation in the CML. The Northern Hemispheric atmospheric $\delta^{14}C$ record shows a 512-yr periodicity (Stuiver and Braziunas, 1993), which is similar to the observed ~500 year periodicity of the beach ridge record during the Pre-

Classic period. Such a centennial scale periodicity is not apparent in Lake Tuspan's diatom record (Fig. 3), nor in any of the other palaeo-precipitation records from the Maya Lowlands (Fig. A2), but has been identified in the Ti record from Lake Juanacatlán in the highlands of Central Mexico (Jones et al., 2015). This periodicity has been related to the intensity of the North Atlantic thermohaline circulation and variations in solar activity (Stuiver and Braziunas, 1993).

The coherence with fluctuations in solar irradiance is most evident during the 850 BCE (2.8 ka) event, related to the Homeric Grand Solar Minimum. At that~~is~~ time, a strong decrease in the total solar irradiance resulted in higher atmospheric ^{14}C production and a change to cooler and wetter conditions in the Northern Hemisphere (e.g. Van Geel et al., 1996), and apparently also a shift to wetter conditions in the CML, evident from our two new palaeo-precipitation records (Fig. 4~~3~~). This correlation should not be used as an analogue for modern precipitation variability, when periods of lower solar activity are associated with lower Usumacinta River discharge and hence less precipitation in the CML (Fig. A8~~9~~). Probably due a more northerly mean position of the ITCZ during the Pre-Classic Period precipitation responded differently to solar forcing then today.

It has previously been suggested that there was a coherent response to ~~A similar precipitation response to~~ the late Holocene southward shift of the ITCZ in~~for~~ both n~~N~~orthern South America and the Maya Lowlands ~~has previously been suggested~~ (Haug et al., 2003), implying that the beach ridge record should be in-phase with the Cariaco Ti record (Haug et al., 2001). Although the Cariaco record indicates large centennial~~-~~scale variability in precipitation over n~~N~~orthern South America (Fig. 4~~3~~), this variability is not significantly correlated with the beach-ridge record. The correlation ~~slightly~~ improved slightly using an updated age-depth model for ~~the~~ Cariaco ~~record~~ (Fig. A9~~10~~), but remains insignificant, probably as a consequence of~~due to~~ uncertainties in the chronological control of both records or because of~~due to~~ a more prominent influence of the Northern Atlantic climatic forcing mechanisms in the Maya Lowlands.

4.3 Precipitation versus human development in the CML

Our records indicate that the Early Pre-Classic period in the CML was relatively dry. During that~~is~~ period, the CML were still sparsely populated by moving hunter-gatherers. It is highly likely that before maize became sufficiently productive to sustain sedentism, the karstic lowlands were less attractive for humans than the coastal wetlands along the Gulf of Mexico and Pacific coast, where natural resources were abundantly present to successfully sustain a hunting/gathering subsistence system (Inomata et al., 2015). Reliance on cultivated crops, most notably maize, rapidly increased after the onset of the Middle Pre-Classic period around 1000 BCE (Rosenswig et al., 2015). Between 1000 and~~–~~ 850 BCE, under still dry conditions, there is evidence for increased maize agriculture in the Pacific flood basin (Rosenswig et al., 2015), and within the Olmec area on~~at~~ the Gulf of Mexico coast (Arnold III, 2009), and maize grains (AMS ^{14}C dated to 875 ± 29 BCE) have been found as far as Ceibal within the CML (Inomata et al., 2015). We speculate that wetter conditions after 850 BCE might have been unfavourable for ~~a~~ further development of intensive agriculture in the CML. This is supported by palynological evidence, indicating that widespread land clearance and agriculture activity did not occur before ~400 BCE (Wahl et al., 2007; Galop et al., 2004; Islebe et al., 1996; Leyden et al., 1987), despite some early local agricultural activity (Wahl et al., 2014; Rushton et al., 2013; McNeil et al., 2010~~; Galop et al., 2004~~). A return to drier conditions during the Late Pre-Classic period coincided with an expansion of maize-based agriculture in the CML, and communities within the Maya Lowlands show ~~a~~ strong and steady development ~~with relatively uniform ceramic and architectural styles~~ (Hansen, 2017; Inomata and Henderson, 2016). Hence, major development of Maya civilization in the Central Maya Lowlands occurred only after the onset of the Late Pre-Classic period, when climate became progressively drier, in line with earlier findings that drier conditions were favourable for agricultural development in the CML (Wahl et al., 2014). Changes in the distribution of rainfall probably also changed, and large floods, most evident during the Archaic and early Pre-Classic period, occurred much less frequently after approximately 1000 BCE.

5. Conclusions

For the first time a regional palaeo-precipitation record has been reconstructed for the Central Maya Lowland (CML), based on an ~~. The~~ exceptionally well dated high resolution beach ridge record. This record indicates centennial scale precipitation fluctuations during the Pre-Classic period that are not always registered in local records, adding valuable new insights into larger scale climatic forcing mechanisms for the CML. The generally poor correlation between the regional and local palaeo-precipitation reconstructions are probably related to spatial precipitation variability, and chronological

uncertainties of many~~the~~ records. Additional research of beach ridge formation processes are~~is~~ needed to extend this regional precipitation reconstruction to the Classic and Post-Classic period.
We have also generated a local scale palaeo-precipitation record using ~~demonstrate the applicability of~~ diatoms preserved in a core from Lake Tuspan, ~~for palaeoprecipitation reconstructions at a local scale,~~ thereby adding an alternative proxy to the relatively high number of local reconstructions predominantly based on oxygen isotope variability. We recognise, however, that diatom preservation is often poor in the carbonate lakes across the wider region. As a result,~~T~~ the correlation between these two reconstructions is variable through time.

~~The generally poor correlation between the regional and local palaeoprecipitation reconstructions are probablylikely related to spatial precipitation variability, and chronological uncertainties of the records.~~

Although the occurrence of a prolonged drought during the end of the Early Pre-Classic period, which we report here, is evident in~~from~~ other~~ many local~~ palaeo-precipitation reconstructions from the CML, the subsequent wet period during the Middle Pre-Classic period, registered in both our new records, is less evident elsewhere~~in other available local records.~~

~~Both our records also indicate the occurrence of a prolonged wet period during the Middle Pre-Classic period~~. ~~, which seems to be related to the Homeric Grand Solar Minimum.~~ Although many researchers have focused on the impact of drought on the development and disintegration of Maya societies, one should consider this prolonged wet period~~s~~ as potentially unfavourable for the development and intensification of agriculture in the CML, particularly in the wetter areas. We cannot be certain about the impact of wetter conditions on the Maya. However, owing to the lack of the development at this time we theorise that the wet period could have created poor growing conditions for maize in the CML. In order to test theory, we advocate for the use of process-based modelling approaches which capture heterogeneous environmental constraints on crop growth for given climate boundary conditions such as the approach applied by Dermody et al. (2014).

~~It seems evident~~Our results provide evidence that North Atlantic atmospheric-oceanic forcing plays an important role in the modulation of the observed centennial scale precipitation variability, however further ~~research~~ studies are required which compare well-dated terrestrial reconstructions that capture regional signals with solar and oceanic reconstructions to gain~~is needed for~~ a better understanding of ~~the~~ climate forcing mechanisms, both in the CML and across the wider region. ~~This is particularly true for periods in the past when climatic responses to apparent forcings appear to be different from those during the instrumental period.~~

Acknowledgements

This research is supported by the Netherlands Organization for Scientific Research (NWO-grant 821.01.007). The LiDAR data was generously provided by INEGI, Mexico. We acknowledge Philippe Martinez, Jacques Giraudeau and Pierre Carbonel for the XRF core scan measurements, and we would like to thank Peter Douglas, Pete Akers and Gerald Haug for providing their data. We thank Konrad Hughen for valuable suggestions to update the age-depth model for Cariaco's sediment core 1002D. We thank Ton Markus for improving the figures, and Mark Brenner and an anonymous reviewer for their valuable comments to improve the paper.

References

Akers, P.D., Brook, G.A., Railsback, L.B., Liang, F., Iannone, G., Webster, J.W., Reeder, P.P., Cheng, H., and Edwards, R.L., An extended and higher-resolution record of climate and land use from stalagmite MC01 from Macal Chasm, Belize, revealing connections between major dry events, overall climate variability, and Maya sociopolitical changes. Palaeogr Palaeoclimatol Palaeoecol 459: 268-288, 2016.

Amador, J.A., Alfaro, E.J., Lizano, O.G., and Magaña, V.O., Atmospheric forcing of the eastern tropical Pacific: A review. Progress in Oceanography 69: 101-142, 2006.

Anselmetti, F.S., Hodell, D.A., Ariztegui, D., Brenner, M., and Rosenmeier, M.F., Quantification of soil erosion rates related to ancient Maya deforestation. Geology 35: 915–918, 2007.

Arnold III, P.J., Settlement and subsistence among the Early Formative Gulf Olmec. J Anthropol Archaeol 28: 397-411, 2009.

Banco Nacional de Datos de Aguas Superficiales, Conagua. http://www.conagua.gob.mx/CONAGUA07/Contenido/Documentos/Portada BANDAS.htm conagua.gob.mx/Bandas/Bases_Datos_Presas/, consulted January 2017.

Bhattacharya, T., Byrne, R., Böhnel, H., Wogau, K., Kienel, U., Ingram, B.L., and Zimmerman, S., Cultural implications of late Holocene climate change in the Cuenca Oriental, Mexico. Proc Natl Acad Sci USA 112(6), 1693–1698, 2015.

Batterbee, R.W., A new method for estimating absolute microfossil numbers with special reference to diatoms. Limnol Oceonogr 18: 647-653, 1973.

Beach, T., Luzzadder-Beach, S., Cook, D., Dunning, N., Kennett, D.J., Krause, S., Terry, R., Trein, D., and Valdez, F., Ancient Maya impacts on the Earth's surface: An Early Anthropocene analog? Quat Sci Rev 124: 1-30, 2015.

Bernal, J.P., Lachniet, M., McCulloch, M., Mortimer, G., Morales, P., and Cienfuegos, E., A speleothem record of Holocene climate variability from southwestern Mexico. Quat Res 75:104–113, 2011.

Bond, G., Kromer, B., Beer, J., Muscheler, R., Evans, M.N., Showers, W., Hoffmann, S., Lotti-Bond, R., Hajdas, I., and Bonani, G., Persistent Solar Influence on North Atlantic Climate During the Holocene. Science 294: 2130-2136, 2001.

Bronk Ramsey, C., Oxcal 4.2.; http://c14.arch.ox.ac.uk/oxcal.html, 2016.

Bronk Ramsey, C., Bayesian analysis of radiocarbon dates. Radiocarbon 51: 337–360, 2009.

Burney, D.A., and Pigott Burney, L., Holocene Charcoal Stratigraphy from Laguna Tortuguero, Puerto Rico, and the Timing of Human Arrival on the Island. J Archaeol Sci 21: 273-281, 1994.

Coe, M.D., The Maya, eight edition, Thames and Hudson, London, UK, 2011.

Curtis, J.H., and Hodell, D.A., Climate Variability on the Yucatan Peninsula (Mexico) during the Past 3500 Years, and Implications for Maya Cultural Evolution. Quat Res 46: 37-47, 1996.

Curtis, J.H., Brenner, M., Hodell, D.A., Balser, R.A., Islebe, G.A., and Hooghiemstra, H., A multiproxy study of Holocene environmental change in the Maya Lowlands of Peten, Guatemala. J Paleolimnol 19: 139–159, 1998.

Czarnecki, D.B., and Blinn, D.W., Observations on Southwestern Diatoms. I. Plagiotropis arizonica N. Sp. (Bacillariophyta, Entomoneidaceae), a large Mesohalobous Diatom. Trans Am Microsc Soc 97: 393-396, 1978.

Davies, S. J., Lamb, H. F., & Roberts, S. J. Micro-XRF Core Scanning in Palaeolimnology: Recent Developments. In Croudace and Rothwell (eds) *Micro-XRF Studies of Sediment Cores,* Springer. pp. 189-226, 2015.

Dermody, B.J., van Beek, R.P.H., Meeks, E., Klein Goldewijk, K., Scheidel, W., van der Velde, Y., Bierkens, M.F.P., Wassen, M.J., Dekker, S.C., ~~2014.~~ A virtual water network of the Roman world. Hydrol. Earth Syst. Sci. 18, 5025–5040, 2014.~~. https://doi.org/10.5194/hess-18-5025-2014~~

Díaz, K.A., Pérez, L., Correa-Metrio, A., Franco-Gaviria, J.F., Echeverria, P., Curtis, J., and Brenner, M., Holocene environmental history of tropical, mid-altitude Lake Ocotalito, México, inferred from ostracodes and non-biological indicators. Holocene 27, 1308-1317, 2017.

Domínguez-Vázquez, G., and Islebe, G.A., Protracted drought during the late Holocene in the Lacandon rain forest, Mexico. Veg Hist Archaeobot 17: 327-333, 2008.

Douglas, P.M.J., Demarest, A.A., Brenner, M., and Canuto, M.A., Impacts of Climate Change on the Collapse of Lowland Maya Civilization. Annu Rev Earth Planet Sci 44: 613–645, 2016.

Douglas, P.M.J., Pagani, M., Canuto, M.A., Brenner, M., Hodell, D.A., Eglinton, T.I., and Curtis, J.H., Drought, agricultural adaptation, and sociopolitical collapse in the Maya Lowlands. Proc Natl Acad Sci USA 112: 5607-5612, 2015.

Dunning, N.P., Beach, T.P., and Luzzadder-Beach, S., Kax and kol: Collapse and resilience in lowland Maya civilization. Proc Natl Acad Sci USA 109(10): 3652–3657, 2012.

Dunning, N.P., McCane, C., Swinney, T., Purtill, M., Sparks, J., Mann, A., McCool, J.-P., and Ivenso, C., Geoarchaeological Investigations in Mesoamerica Move into the 21st Century: A Review. Geoarchaeology 30: 167–199, 2015.

Ebert, C.E., Peniche May, N., Culleton, B.J., Awe, J.J., and Kennett, D.J., Regional response to drought during the formation and decline of PreClassic Maya societies. Quat Sci Rev 173, 211-235, 2017.

Fleury, S., Malaizé, B., Giraudeau, J., Galop, D., Bout-Roumazeilles, V., Martinez, P., Charlier, K., Carbonel, P., and Arnauld, M.-C., Impacts of Mayan land use on Laguna Tuspan watershed (Petén, Guatemala) as seen through clay and ostracode analysis. J Archaeol Sci 49: 372–382, 2014.

Ford, A., and Nigh, R., The Maya Forest Garden: Eight Millennia of Sustainable Cultivation of the Tropical Woodland, Taylor and Francis, London, New York, 2015.

Galop, D., Lemonnier, E., Carozza, J.M., and Metailie, J.P., Bosques, milpas, casas y aguadas de antaño. In: La Joyanca, ciudad maya del noroeste del Peten (Guatemala), Arnauld C. et Breuil-Martinez V. (eds.). CEMCA, CIRMA, Associacion Tikal, Guatemala, 55-71, 2004.

Gasse, F., Juggins, S., and Ben Khelifa, L., Diatom-based transfer functions for inferring past hydrochemical characteristics of African lakes. Palaeogeogr Palaeoclimatol Palaeoecol 117: 31-54, 1995.

Grinsted, A., Moore, J.C., and Jevrejeva, S., Application of the cross wavelet transform and wavelet coherence to geophysical time series. Nonlinear Processes Geophys 11: 561-566, 2004.

Hansen, R.D., The Feast Before Famine and Fighting: The Origins and Consequences of Social Complexity in the Mirador Basin, Guatemala. Feast, Famine or Fighting? Multiple Pathways to Social Complexity, Chacon, R.J., and Mendoza, R.G. (eds), Springer, Dordrecht, the Netherlands, pp 305-335, 2017.

Haug, G.H., Hughen, K.A., Sigman, D.M., Peterson, L.C., and Röhl, U., Southward Migration of the Intertropical Convergence Zone Through the Holocene. Science 293, 1304–1308, 2001.

Haug, G.H., Gunther, D., Peterson, L.C., Sigman, D.M., Hughen, K.A., and Aeschlimann, B., Climate and the Collapse of Maya Civilization. Science 299: 1731-1735, 2003.

Hijmans, R.J., Cameron, S.E., Parra, J.L., Jones, P.G., and Jarvis, A., Very high resolution interpolated climate surfaces for global land areas. Int J of Clim 25: 1965-1978, 2005.

Hodell, D.A., Brenner, M., and Curtis, J.H., Climate and cultural history of the Northeastern Yucatan Peninsula, Quintana Roo, Mexico. Climatic Change 83: 215–240, 2007.

Hodell D.A., Brenner, M., and Curtis, J.H., Terminal Classic drought in the northern Maya lowlands inferred from multiple sediment cores in Lake Chichancanab (Mexico). Quat Sci Rev 24: 1413–1427, 2005.

Hodell, D.A., Brenner, M., Curtis, J.H., and Guilderson, T., Solar forcing of drought frequency in the Maya lowlands. Science 292: 1367–1369, 2001.

Hodell, D.A., Curtis, J.H., and Brenner, M., Possible role of climate in the collapse of Classic Maya civilization. Nature 375: 391–394, 1995.

Hoggarth, J.A., Breitenbach, S.F.M., Culleton, B.J., Ebert, C.E., Mason, M.A., and Kennett, D.J., The political collapse of Chichén Itzá in climatic and cultural context. Glob Planet Change 138: 25-42, 2016.

Iannone, G., The Great Maya Droughts in Cultural Context: Case Studies in Resilience and Vulnerability, Univ Press of Colorado, Boulder, CO, USA, 2014.

Inomata, T., and Henderson, L., Time tested: re-thinking chronology and sculptural traditions in Preclassic southern Mesoamerica. Antiquity 90: 456-471, 2016.

Inomata, T., MacLellan, J., Triadan, D., Munson, J., Burham, M., Aoyama, K., Nasu, H., Pinzón, F., and Yonenobu, H., Development of sedentary communities in the Maya lowlands: Coexisting mobile groups and public ceremonies at Ceibal, Guatemala. Proc Natl Acad Sci USA 112: 4268–4273, 2015.

Islebe, G.A., Hooghiemstra, H., Brenner, M., Curtis, J.H., and Hodell, D.A., A Holocene vegetation history from lowland Guatemala. Holocene 6: 265–271, 1996.

Jones, M.D., Metcalfe, S.E., Davies, S.J., and Noren, A., Late Holocene climate reorganisation and the North American Monsoon. Quat Sci Rev 124: 290-295, 2015.

Kalnay E., Kanamitsu, M., Kistler, R., Collins, W., Deaven, D., Gandin, L., Iredell, M., Saha, S., White, G., Woollen, J., Zhu, Y., Chelliah, M., Ebisuzaki, W., Higgins, W., Janowiak, J., Mo, K.C., Ropelewski, C., Wang, J., Leetmaa, A., Reynolds, R., Jenne, R., and Joseph, D., The NCEP/NCAR Reanalysis 40-year Project. Bull Am Meteorol Soc 77: 437–471, 1996.

Kennett, D.J., Breitenbach, S.F.M., Aquino, V.V., Asmerom, Y., Awe, J., Baldini, J.U.L., Bartlein, P., Culleton, B.J., Ebert, C., Jazwa, C., Macri, M.J., Marwan, N., Polyak, V., Prufer, K.M., Ridley, H.E., Sodemann, H., Winterhalder, B., and Haug, G.H., Development and disintegration of Maya political systems in response to climate change. Science 338: 788–791, 2012.

Kopp, G., and Lean, J.L., A new, lower value of total solar irradiance: Evidence and climate significance. Geophys Res Lett 38: L01706, 2011.

Krivova, N.A., Balmaceda, L., and Solanki, S.K., Reconstruction of solar total irradiance since 1700 from the surface magnetic flux. Astron Astrophys 467: 335–346, 2007.

Lachniet, M.S., Asmerom, Y., Bernal, J.P., Polyak, V., and Vazquez-Selem, L., Orbital pacing and ocean circulation-induced collapses of the Mesoamerican monsoon over the past 22,000 y. Proc Natl Acad Sci USA 110: 9255–9260, 2013.

Lachniet, M.S., Asmerom, Y., Polyak, V., and Bernal, J.P., Two millennia of Mesoamerican monsoon variability driven by Pacific and Atlantic synergistic forcing. Quat Sci Rev 155: 100-113, 2017.

Lee, S., Gaiser, E., VanDeVijver, B., Edlund, M.B., and Spaulding, S.A., Morphology and typification of *Mastogloia smithii* and *M. lacustris*, with descriptions of two new species form the Florida Everglades and the Caribbean region. Diatom research 29: 325-350, 2014.

Lentz, D.L., Dunning, N.P., Scarborough, V.L., Magee, K.S., Thompson, K.M., Weaver, E., Carr, C., Terry, R.E., Islebe, G., Tankersley, K.B., Grazioso Sierra, L., Jones, J.G., Buttles, P., Valdez, F., and

Ramos Hernandez, C.E., Forests, fields, and the edge of sustainability at the ancient Maya city of Tikal. Proc Natl Acad Sci USA 111: 18513–18518, 2014.

Leyden. B.W., Man and Climate in the Maya Lowlands. Quat Res 28: 407-414, 1987.

Lohse, J., Archaic Origins of the Lowland Maya. Latin American Antiquity 21: 312-352, 2010.

McNeil, C.L., Burney, D.A., and Burney, L.P., Evidence disputing deforestation as the cause for the collapse of the ancient Maya polity of Copan, Honduras. Proc Natl Acad Sci USA 107: 1017–1022, 2010.

Medina-Elizalde, M., Burns, S.J., Polanco-Martinez, J.M., Beach, T., Lases-Hernandez, F., Shen, C.C., and Wang, H.C., High-resolution speleothem record of precipitation from the Yucatan Peninsula spanning the Maya Preclassic Period. Glob Planet Change 138: 93-102, 2016.

Medina-Elizalde, M., Burns, S.J., Lea, D.W., Asmerom, Y., von Gunten, L., Polyak, V., Vuille, M., and Karmalkar, A., High resolution stalagmite climate record from the Yucatan Peninsula spanning the Maya terminal classic period. Earth Planet Sci Lett 298: 255–262, 2010.

Metcalfe, S.E., Barron, J.A., and Davies, S.J., The Holocene history of the North American Monsoon: 'known knowns' and 'known unknowns' in understanding its spatial and temporal complexity. Quat Sci Rev 120: 1-27, 2015.

Metcalfe, S., Breen, A., Murray, M., Furley, P., Fallick, A., and McKenzie, A., Environmental change in northern Belize since the latest Pleistocene. J Quat Sci 24: 627-641, 2009.

Mueller, A.D., Islebe, G.A., Hillesheim, M.B., Grzesik, D.A., Anselmetti, F.S., Ariztegui, D., Brenner, M., Curtis, J.H., Hodell, D.A., and Venz, K.A., Climate drying and associated forest decline in the lowlands of northern Guatemala during the Holocene. Quat Res 71: 133-141, 2009.

Nooren, K., Hoek, W.Z., Van der Plicht, H., Sigl, M., Van Bergen, M.J., Galop, D., Torrescano-Valle, N., Islebe, G., Huizinga, A., Winkels, T., and Middelkoop, H., Explosive eruption of El Chichón volcano (Mexico) disrupted 6th century Maya civilization and contributed to global cooling. Geology 45: 175-178, 2017a.

Nooren, K., Hoek, W.Z., Winkels, T., Huizinga, A., Van der Plicht, H., Van Dam, R.L., Van Heteren, S., Van Bergen, M.J., Prins, M.A., Reimann, T., Wallinga, J., Cohen, K.M., Minderhoud, P., and Middelkoop, H., The Usumacinta-Grijalva beach-ridge plain in southern Mexico: a high-resolution archive of river discharge and precipitation. Earth Surf Dynam 5: 529-556, 2017b.

Novelo, E., Tavera, R., and Ibarra, C., Bacillariophyceae from karstic wetlands in Mexico, J. Cramer, Berlin, Germany, 2007.

Paillès, C., Sylvestre, F., Escobar, J., Tonetto, A., Rustig, S., and Mazur, J-C, *Cyclotella petenensis* and *Cyclotella cassandrae*, two new fossil diatoms from Pleistocene sediments of Lake Petén-Itzá, Guatemala, Central America. Phytotaxa 351: 247-263, 2018.

Patrick, R., and Reimer, C.W., Diatoms of the United States, Vol. I, Monograph 13, Acad Nat Sci, Philadelphia, USA, 1966.

Patrick, R., Reimer, C.W., Diatoms of the United States, Vol. II, Part1, Monograph 13, Acad Nat Sci, Philadelphia, USA. 1975.

Pollock, A.L., Van Beynen, P.E., De Long, K.L., Polyak, V., Asmerom, Y., and Reeder, P.P., A mid-Holocene paleoprecipitation record from Belize. Palaeogeogr Palaeoclimatol Palaeoecol 463: 103-111, 2016.

Reed, J.M., A diatom-conductivity transfer function for Spanish salt lakes. J Paleolimnol 19: 399-416, 1998.

Reimer, P.J., Bard, E., Bayliss, A., Warren Beck, J., Blackwell, P.G., Ramsey, C.B., Buck, C.E., Cheng, H., Lawrence Edwards, R., Friedrich, M., Grootes, P.M., Guilderson, T.P., Haflidason, H., Hajdas, I., Hatté, C., Heaton, T.J., Hoffmann, D.L., Hogg, A.G., Hughen, K.A., Felix Kaiser, K., Kromer, B., Manning, S.W., Niu, M., Reimer, R.W., Richards, D.A., Marian Scott, E., Southon, J.R., Staff, R.A, Turney, C.S.M., and Van der Plicht, J., IntCal13 and Marine13 radiocarbon age calibration curves 0–50,000 years cal BP. Radiocarbon 55: 1869–1887, 2013.

Rosenmeier, M.F., Hodell, D.A., Brenner, M., Curtis, J.H., and Guilderson, T.P., A 4000-year lacustrine record of environmental change in the southern Maya lowlands, Peten, Guatemala. Quat Res 57: 183–190, 2002.

Rosenswig, R.M., VanDerWarker, A.M., Culleton, B.J., and Kennett, D.J., Is it agriculture yet? Intensified maize-use at 1000 cal BC. in the Soconusco and Mesoamerica. J Antropol Archaeol 40: 89-108, 2015.

Rushton, E.A.C., Metcalfe, S.E., and Whitney, B.S.W., A late-Holocene vegetation history from the Maya Lowlands, Lamanai, Northern Belize. Holocene 23: 485-493, 2013.

Schneider, T., Bischoff, T., and Haug, G.H., Migrations and dynamics of the intertropical convergence zone. Nature 513: 45-53, 2014.

Schüpbach, S., Kirchgeorg, T., Colombaroli, D., Beffa, G., Radaelli, M., Kehrwald, N.M., and Barbante, C., Combining charcoal sediment and molecular markers to infer a Holocene fire history in the Maya Lowlands of Petén, Guatemala. Quat Sci Rev 115: 123-131, 2015.

Steinhilber, F. Abreu, J.A., Beer, J., Brunner, I., Christl, M., Fischer, H., Heikkilä, U., Kubik, P.W., Mann, M., McCracken, K.G., Miller, H., Miyahara, H., Oerter, H., and Wilhelms, F., 9,400 years of cosmic radiation and solar activity from ice cores and tree rings. Proc Natl Acad Sci USA 109: 5967–5971, 2012.

Stuiver, M., and Braziunas, T.F., Sun, ocean, climate and atmospheric $^{14}CO_2$: an evaluation of causal and spectral relationships. Holocene 3: 289-305, 1993.

Tankersley, K.B., Dunning, N.P., Scarborough, V., Huff, W.D., Lentz, D.L., and Carr, C., 2016, Catastrophic volcanism and its implication for agriculture in the Maya Lowlands: J Archaeol Sci 5, 465–470, 2016.

Thompson, J.E.S., A Commentary on the Dresden Codex, Am Philosophical Society, Philadelphia, USA, 1972.

Torrescano-Valle, N., and Islebe, G.A., Holocene paleoecology, climate history and human influence in the southwestern Yucatan Peninsula. Rev Palaeobot Palynol 217: 1-8, 2015.

Turner II, B.L., and Sabloff, J.A., Classic Period collapse of the Central Maya Lowlands: Insights about human-environment relationships for sustainability. Proc Natl Acad Sci USA 109: 13908–13914, 2012.

USGS, Shuttle Radar Topography Mission (SRTM) 1 Arc-Second Global dataset. https://lta.cr.usgs.gov/SRTM1Arc, 2009.

Valásquez Garciá, E., The Maya Flood Myth and the Decapitation of the Cosmic Caiman. The PARI Journal 7: 1-10, 2006.

Van Geel, B., Buurman, J., and Waterbolk, H.T., Archaeological and palaeoecological indications for an abrupt climate change in The Netherlands and evidence for climatological teleconnections around 2650 BP. J Quat Sci 11: 451–460, 1996.

Velez, M.I., Curtis, J.H., Brenner, M., Escobar, J., Leyden, B.W., and Popenoe de Hatch, M., Environmental and Cultural Changes in Highland Guatemala Inferred from Lake Amatitlán Sediments. Geoarchaeology 26: 1-19, 2011.

Wahl, D., Byrne, R., and Anderson, L., An 8700 year paleoclimate reconstruction from the southern Maya lowlands. Quat Sci Rev 103: 19–25, 2014.

Wahl, D., Byrne, R., Schreiner, T., and Hansen, R., Palaeolimnological evidence of late-Holocene settlement and abandonment in the Mirador Basin, Peten, Guatemala. Holocene 17: 813-820, 2007.

Figure captions

Figure 1: The image on page 74 of the Codex Dresden depicts a torrential downpour probably associated with a destructive flood (Thompson, 1972).

Figure 2: A large part of the Central Maya Lowlands (outlined with a red dashed line) is drained by the Usumacinta (Us.) River (A). During the Pre-Classic period this river was the main supplier of sand contributing to the formation of the extensive beach ridge plain at the Gulf of Mexico coast (B). Periods of low rainfall result in low river discharges and are associated with relatively elevated beach ridges. The extent~~d~~ of the watersheds of the Usumacinta and Dulce River is calculated from SRTM 1-arc data (USGS, 2009). Indicated are archaeological sites (squares) and proxy records discussed in the text; Tu= Lake Tuspan, Ch = Lake Chichancanab, PI = Lake Peten-Itza, MC = Macal Chasm Cave, and PA = Lago Puerto Arturo.

Figure 3: Summarized proxy record of Lake Tuspan sediment core C. In the lithological column black lines represent large flood layers and grey boxes turbidites. Ca and Si (in cps = counts per second) are presented here as % of total counts. Vertical lines (red) in the (amorphous) Si graphs indicate the one-standard-deviation threshold above the mean. For the diatom record only the relative abundance of 'key' diatom species are shown here. *Denticula elegans* and *Nitzschia amphibia* were excluded from the diatom sum. Notice abrupt change around 11~~0~~00 BCE.

Figure 4~~3~~: Comparison of the Lake Tuspan and beach ridge record (A) with local and proximal records from Macal-Chasm cave (Akers et al., 2016) and the Cariaco basin (Haug et al., 2001)(B). We used an updated age-depth model for t~~T~~he Cariaco record ~~is conform updated age-depth model~~ (Fig. A9~~10~~). Climate records related to North Atlantic atmospheric-oceanic forcing are indicated in panel C, including the drift ice reconstruction from the North Atlantic (Bond et al., 2001), the Northern Hemispheric residual atmospheric $\delta^{14}C$ content (Reimer et al., 2013), the Northern-to Southern hemispheric temperature anomaly (Schneider et al., 2014) and reconstructed Total Solar Irradiance (TSI) (Steinhilber et al., 2012).

Figure 5~~4~~:Wavelet Transform Coherence (WTC) analysis between the beach ridge record and the Northern Hemispheric atmospheric $\delta^{14}C$ record (Reimer et al., 2013)(A) and the North Atlantic ice drift record (Bond et al., 2001)(B). The beach ridge record is significantly in anti-phase with both records at approximately 500~~-~~yr time scale, indicating an important role of North Atlantic atmospheric-oceanic forcing on precipitation in the Maya Lowlands during the Pre-Classic period. The 5% significance level against red noise is shown as a thick contour. Arrows indicate phase difference, with in-phase relationship between records if arrows point to the right.

Appendix: Additional figures

Figure A1: Location of proxy records indicated in figure A2 and/or mentioned in the main text. A: Northern Maya Lowlands (Tz=Tzabnah, PL=Punta Laguna, RS=Rio Secreto, Ch=Chichancanab and Si=Silvituc), the Central and Southern Maya Lowlands (PA=Puerto Arturo, NRL=New River Lagoon, Tu=Tuspan, PI/Sa=Peten-Itza and Salpeten, MC/CH=Macal Chasm and Chen Ha, and YB=Yok Balum), the Maya Highlands (Oc/Na= Ocotalito and Naja, Am=Amatitlan, and Pet=Petapilla). B: Central Mexico (Jua=Juanacatlan, CdD=Cueva de Diablo, Jx=Juxtlahuacan, and Alj=Aljojuca) and the marine record from the Cariaco (C) basin. Annual precipitation (1950-2000) calculated with WorldClim version 1.4 (release3); Hijmans et al.~~,~~ (2005). Long~~-~~term (1958-1998) mean ITCZ position and wind at 925 hPa ($m.s^{-1}$) for July after Amador et al. (2006), based on NCED/NCAR Reanalysis data (Kalnay et al., 1996).

Figure A2a: Palaeoprecipitation records from the Central Maya Lowlands and Yucatan; Beach ridge elevation and Tuspan diatom record (this study), compiled record of Central Peten and Yucatan (Douglas et al., 2016), Salpeten and Chichancanab dD wax-corr. (Douglas et al., 2015), Salpeten δ^{18}O (Rosenmeier et al., 2012), Peten-Itza δ^{18}O (Curtis et al., 1998), Puerto Arturo δ^{18}O (Wahl et al., 2014), Macal Chasm δ^{18}O (Akers et al., 2016), Chen Ha δ^{18}O (Pollock et al., 2016), Yok Balum δ^{18}O (Kennett et al., 2012), Rio Secreto δ^{18}O (Medina-Elizalde et al., 2016), Silvituc DV-pollen (Torrescano-Valle and Islebe, 2015), Chichancanab S and δ^{18}O (Hodell et al., 1995), Punta Laguna δ^{18}O (Hodell et al., 2007), and Tzabnah δ^{18}O (Medina-Elizalde et al., 2010). Notice that the y-axis is sometimes reversed, so that excursions above the x-axis always indicate relatively drier conditions.

Figure A2b: Proxy records from the Central Maya Lowlands, the Maya Highlands and Central Mexico. Peten-Itza charcoal (Schüpbach et al., 2015), Peten-Itza pollen (Islebe et al., 1996), Amatitlan *Aulacoseira* and *Pinus* (Velez et al., 2011), Petapilla *Pinus* (McNeil et al., 2010), Naja *Pinus* (Domínguez-Vázquez and Islebe, 2008), Ocotalito Sr (Díaz et al., 2017), Aljojuca δ^{18}O (Bhattacharya et al., 2015), Cueva del Diablo δ^{18}O (Bernal et al., 2011), Juxtlahuaca δ^{18}O (Lachniet et al., 2015, 2017), and Juanacatlan Ti ~~-~~15-~~-~~point running mean (Jones et al., 2015).

Figure A3: Age-distance model for beach ridge transect B~~ (after Nooren et al., 2017b)~~. ~~The age distance model is based on 35 AMS ^{14}C dated terrestrial macro-remains (mainly leaf fragments isolated from organic debris layers), and 20 OSL dated sand samples (determined on small aliquots of quartz grains).~~ We refer to Nooren et al. (2017b) for further details.

~~Figure A4: Summarized proxy record of Lake Tuspan sediment core C. The 1-4 cm thick dark palaeoflood layers contrast with the predominantly light coloured calcareous deposits, and are characterized by elevated detrital input, resulting in elevated concentrations of Si (cps = counts per second), amorphous silica (% of dry weight), and charred plant fragments (number of particles/g dw). Only the relative abundance of ‘key’ diatom species are shown here and the small and often dominant *Denticula elegans* and *Nitzschia amphibia* species were excluded from the diatom sum. The first Principal Component axis (PC-1) is interpreted as a lake water salinity indicator, with low values corresponding to high salinity waters, reflecting relatively dry conditions. Notice abrupt change around 1000 BCE.~~

Figure A4~~5~~: Diatom record for lake Tuspan core C. Diatom concentrations (*1000 valves/g dw) were determined on 37 selected 1-cm samples and diatom percentages (only the ‘key species’ are shown here) were determined on the 123 subsamples at 4-12-~~-~~cm contiguous intervals. The small and often dominant *Denticula elegans* and *Nitzschia amphibia* species were excluded from the diatom sum.

Figure A5~~6~~: Detailed diatom record around one of the larger flood events ~1200 BCE.

Figure A6~~7~~: Age-depth model for Tuspan core C. The age-depth model is based on a linea~~i~~r interpolation between calibrated ages of radiocarbon dated terrestrial macroremains from core A (Galop et al., 2004) and core C (Fleury et al., 2014). The model is most reliable for ages between ~2500 BCE and 1000 CE.

Figure A7~~8~~: Wavelet Transform Coherence (WTC) analysis between the beach ridge record and the Macal Chasm δ^{18}O record (Akers et al., 2016). The 5% significance level against red noise is shown as a thick contour. Arrows indicate phase difference, with in-phase relationship between records if arrows point to the right.

Figure A8~~9~~: Mean annual discharge of the Usumacinta river at Boca del Cerro (Banco Nacional de Datos de Aguas Superficiales, consulted in January 2017) compared with the total solar irradiance (TSI). The TSI is comprised of the reconstruction from 1700-2004 (Krivovo at al., 2007), concatenated with observations from the Total Irradiance Monitor (TIM) on NASA's Solar Radiation and Climate Experiment (SORCE) from 2005-2011 (Kopp and Lean, 2011). 4.56 watts are added to the TIM measurements as previous reconstructions were calibrated against less accurate measuring equipment, compared with the TIM instrument, which led to an overestimation of TSI.

Figure A9~~10~~: Updated age-depth model for Cariaco core 1002D. Original model (Haug et al., 2001) has been based on a linea~~i~~r interpolation of calibrated ages. We applied a 4th-~~-~~order polynomal fit through modelled ages calculated with a P_sequence model (Oxcal 4.2) (Bronk Ramsey, 2009, 2016):

k = 10, Marine13 calibration curve, delta R = 15 ± 50, one outlier: NSRL-13050.

Climate impact on the development of Pre-Classic Maya civilization

Authors
Kees Nooren[1], Wim Z. Hoek[1], Brian J. Dermody[1,2], Didier Galop[3], Sarah Metcalfe[4], Gerald Islebe[5] and Hans Middelkoop[1].

Affiliations
[1]Utrecht University, Faculty of Geosciences, 3508 TC Utrecht, The Netherlands;
[2]Utrecht University, Copernicus Institute of Sustainable Development, 3508 TC Utrecht, The Netherlands;
[3]Université Jean Jaurès, CNRS, UMR 5602 GEODE, 31058 Toulouse, France;
[4]University of Nottingham, School of Geography, Nottingham NG7 2RD, UK
[5]El Colegio de la Frontera Sur, Unidad Chetumal Herbario, Chetumal, AP 424 Quintana Roo, Mexico;

Correspondence to: Kees Nooren (k.nooren@gmail.com)

Keywords
Pre-Classic Maya period, Central Maya Lowlands, climate record, beach ridges, palaeo-precipitation, 500-yr periodicity, 2.8 ka event.

Abstract
The impact of climate change on the development and disintegration of Maya civilization has long been debated. The lack of agreement among existing palaeoclimatic records from the region has prevented a detailed understanding of regional-scale climatic variability, its climatic forcing mechanisms, and its impact on the ancient Maya. We present two new palaeo-precipitation records for the Central Maya Lowlands, spanning the Pre-Classic period (1800 BCE – 250 CE), a key epoch in the development of Maya civilization. A beach ridge elevation record from world's largest late Holocene beach ridge plain provides a regional picture, while Lake Tuspan's diatom record is indicative of precipitation changes at a local scale. We identify centennial-scale variability in palaeo-precipitation that significantly correlates with the North Atlantic $\delta^{14}C$ atmospheric record, with a comparable periodicity of approximately 500 years, indicating an important role of North Atlantic atmospheric-oceanic forcing on precipitation in the Central Maya Lowlands. Our results show that the Early Pre-Classic period was characterized by relatively dry conditions, shifting to wetter conditions during the Middle Pre-Classic period, around the well-known 850 BCE (2.8 ka) event. We propose that this wet period may have been unfavorable for agricultural intensification in the Central Maya Lowlands, explaining the relatively delayed development of Maya civilization in this area. A return to relatively drier conditions during the Late Pre-Classic period coincides with rapid agricultural intensification in the region and the establishment of major cities.

1. Introduction

During the last decades, a wealth of new data has been gathered to understand human-environmental interaction and the role of climate change in the development and disintegration of societies in the Maya Lowlands (e.g., Akers et al., 2016; Douglas et al., 2015, 2016; Dunning et al., 2012, 2015; Lentz et al., 2014; Turner and Sabloff, 2012). Previous studies have emphasized the impact of prolonged droughts and their possible link with social downturn, such as the Pre-Classic Abandonment and the Classic Maya Collapse (Ebert et al., 2017; Hoggarth et al., 2016; Lentz et al., 2014; Kennett et al., 2012; Medina-Elizalde et al., 2010, 2016; Haug et al., 2003; Hodell et al., 1995, 2001, 2005). Less attention has been given to episodes of excessive rain and floods that may also have severely impacted ancient Maya societies (e.g. Iannone et al., 2014). Evidence for such impacts is found in the fact that floods, as well as droughts, are an important theme depicted in the remaining ancient Maya codices (Fig. 1) (Thompson, 1972), and Maya mythological stories (Valásquez Garciá, 2006).

One of the main challenges in palaeoclimatic reconstructions is to unravel climate from human induced changes. Maya societies played a key role in the formation of the landscape, but the degree of human induced impact remains highly debated (Hansen, 2017; Beach et al., 2015; Ford and Nigh, 2015). For example, it is proposed that the increase in sedimentation rate after 1000 BCE at Lake Salpeten (Anselmetti et al., 2007) and Peten-Itza (Mueller et al., 2009) is related to human induced soil erosion. However, other high resolution lake records from the area do not show a significant increase in sedimentation rate during the Pre-Classic or Classic period (e.g. Wahl et al., 2014), and past volcanic activity could have been responsible for the deposition of smectite rich clay layers in inland lakes

(Tankersley et al., 2016; Nooren et al., 2017a). Palynological records from the Central Maya Lowlands (CML, Fig. 2) show no evidence of widespread land clearance and agriculture before ~400 BCE (Wahl et al., 2007; Islebe et al., 1996; Leyden et al., 1987), and there is growing consensus that the decline in the percentage of lowland tropical forest pollen during the Pre-Classic period (Galop et al., 2004; Islebe et al., 1996; Leyden et al, 1987) was caused by climatic drying instead of deforestation (Torrescano and Islebe, 2015; Wahl et al., 2014; Mueller et al., 2009).

In this paper, we present two new palaeo-precipitation records reflecting precipitation changes in the CML. The records span the Pre-Classic period (1800 BCE – 250 CE), when Maya societies in the CML transformed from predominantly mobile hunter-gatherers in the Early Pre-Classic period (e.g. Inomata et al., 2015; Coe, 2011; Lohse, 2010), to complex sedentary societies that founded impressive cities like El Mirador by the later part of the Pre-Classic period (Hansen, 2017; Inomata and Henderson, 2016). The period of rapid growth in these centralized societies probably occurred much later than previously thought, sometime after the start of the Late Pre-Classic period around 400 BCE (Inomata and Henderson, 2016). This raises the question for the reason behind the delayed development of societies in this area, which was to become the core area of Maya civilization during the following Classic period (250 – 900 CE). There is recent evidence that climate during the Middle Pre-Classic Period (1000 – 400 BCE) may have been less stable than recently reported (Ebert et al., 2017). We propose that anomalously wet conditions could have been unfavourable for the intensification of maize-based agriculture, which formed the underlying subsistence economy responsible for the development of many neighbouring Mesoamerican societies during this period.

The CML have been intensively studied, and several well-dated speleothem, palynological, and limnological records have been obtained for this area (Díaz et al., 2017; Akers et al., 2016; Douglas et al.; 2015; Wahl et al., 2014; Kennett et al., 2012; Mueller et al., 2009; Metcalfe et al., 2009; Domínguez-Vázquez and Islebe, 2008; Galop et al., 2004; Rosenmeier et al., 2002; Islebe et al., 1996) (Fig. 2 and A1). However, palaeo-precipitation signals from these records and those from adjacent areas in the Yucatan and Central Mexico exhibit large differences among records (Fig. A2), making the reconstruction and interpretation of larger-scale precipitation for the region a challenge (Lachniet et al., 2013, 2017; Douglas et al., 2016; Metcalfe et al., 2015). Existing climate reconstructions mostly represent local changes and are predominantly based on oxygen isotope variability, although some new proxies have been introduced recently (e.g. Díaz et al., 2017; Douglas et al., 2015).

We present a regional-scale palaeo-precipitation record for the CML, extracted from world's largest late Holocene beach ridge sequence at the Gulf of Mexico coast (Fig. 2B). The beach ridge record captures changes in river discharge resulting from precipitation patterns over the entire catchment of the Usumacinta River and thus represents regional changes in precipitation over the CML (Nooren et al., 2017b). Currently the annual discharge of the Usumacinta river is approximately 2000 m^3/s, corresponding to ~40 % of the excess or effective rain falling in the 70,700 km^2 large catchment (Nooren et al., 2017b). Mean annual precipitation within the catchment is ~2150 mm, with 80 % falling during the boreal summer, related to the North American or Mesoamerican Monsoon system (Lachniet et al., 2013, 2017; Metcalfe et al., 2015). The interpretation of the beach ridge record is supported by a new multi-proxy record from Lake Tuspan, an oligosaline lake situated within the CML. The lake receives most of its water from a relatively small catchment of 770 km^2 (Fig. 2) and hence provides a local precipitation record, to complement the regional signal from the beach ridge sequence.

Regional palaeo-precipitation signal

The coastal beach ridges consist of sandy material originating from the Grijalva and Usumacinta rivers, topped by wind-blown beach sand (Nooren et al., 2017b). Although multiple factors determine the final elevation of the beach ridges, it has been shown that during the period 1775 ± 95 BCE to 30 ± 95 CE (at 1σ), roughly coinciding with the Pre-Classic period, beach ridge elevation was primarily determined by the discharge of the Usumacinta river. Low elevation anomalies of the beach ridges occur in periods with increased river sediment discharge, which in turn is the product of high precipitation within the river catchment. Under these conditions, beach ridges develop relatively rapidly, and are exposed to wind for a shorter period. In contrast, during periods of drought, sediment supply to the coast is reduced, resulting in a decreased seaward progradation rate of the beach ridge plain. This leaves a longer period for aeolian accretion on the beach ridges near the former shoreline, resulting in higher beach ridges (Nooren et al., 2017b). Hence, variations in beach ridge elevation reflect changes in rainfall over the Usumacinta catchment, and thereby represent catchment-aggregated precipitation, rather than a local signal. The very high progradation rates and the very robust age-distance model

(Fig. A3), with uncertainties of the calibrated ages not exceeding 60–70 years (at 1σ), effectively allow the reconstruction of palaeo-precipitation at centennial time scales.

Local palaeo-precipitation signal: Lake Tuspan record

During dry periods, a reduced riverine input of fresh water and a lowering of the lake level enhance the effect of evaporation and increase the salinity of the lake water. Diatom communities within oligo- to hypersaline lakes are strongly influenced by lake water salinity (Reed, 1998; Gasse et al., 1995), and we therefore determined diatom assemblage changes within the Lake Tuspan sediment record (Fig. 3) to reconstruct palaeo-salinities of the lake water, reflecting palaeo-precipitation in the lake's catchment via changes in the balance of precipitation - evaporation.

2. Methods

Beach ridge sequence

Beach ridges elevations were extracted from a Digital Elevation Model (DEM) of the coastal plain along the transects indicated in Fig. 2 (Nooren et al., 2017b). The DEM is based on LiDAR data originally acquired in April-May 2008 and processed by Mexico's National Institute of Statistics and Geography (INEGI), Mexico. The relative beach ridge elevation is defined as the difference between the beach ridge elevation and the long-term (~500 yr) running mean (Fig. A3). The age distance model is based on 35 AMS ^{14}C dated terrestrial macro-remains (mainly leaf fragments isolated from organic debris layers), and 20 OSL dated sand samples (determined on small aliquots of quartz grains) (Nooren et al., 2017b).

Lake Tuspan

Two parallel cores, Tuspan cores B and C, were taken with a Russian corer (type GYK) in shallow water near the inflow of the Rio Dulce (not to be confused with the Rio Dulce that drains lake Izabal in eastern Guatemala), not far from core A which has been studied for pollen (Galop et al., 2004). Semi-quantitative analyses of Si, S, K, Ca, Ti, Mn and Fe were conducted on both cores with an X-ray fluorescence core scanner (type AVAATECH) at 0.5 cm intervals. Deposits of large floods were identified on the basis of elevated concentrations of Si, Fe, Ti and Al (Davies et al., 2015), with peak concentrations exceeding a one-standard-deviation threshold above the mean.

Core C was investigated for amorphous silica, charred plant fragments, and diatoms (Fig. 3, A4 and A5). The core was subsampled at 4-12 cm contiguous intervals, each interval representing 25-80 years. In addition, 37 1-cm samples (representing ~6.5 yr) were processed using the method outlined by Battarbee (1973) to determine diatom concentrations and short term variability (decadal scale). Subsamples were treated with HCl (10 %) to remove calcium carbonate. Large organic particles were removed by wet sieving (250 µm mesh), and charred plant fragments > 250 µm were counted under a dissection microscope. Remaining organic material was removed by heavy liquid separation using a sodiumpolywolframate solution with a density of 2.0 g/cm^3. A silicious residue, denoted 'amorphous silica' was subsequently removed by heavy liquid separation using a sodiumpolywolframate solution with a density of 2.3 g/cm^3, and dry weight was determined after drying of the samples at 105^{o}C.

Slides were prepared from the remaining material. Diatoms were identified, counted and reported as percentages of the total diatom sum, excluding the small and often dominant *Denticula elegans* and *Nitzschia amphibia* species. These species show a large variability on short time scales (Fig. A5), and are not indicative for changes at centennial time scale. We relate changes in diatom assemblages mainly to lake water salinity changes. The first principal component on the entire assemblage (PC-1) is interpreted as a palaeosalinity indicator. Diatom taxonomy is mainly after Patrick and Reimer (1966; 1975) and Novelo, Tavera, and Ibarra (2007). We identified *Plagiotropis arizonica* following Czarnecki and Blinn (1978), *Mastogloia calcarea* following Lee et al. (2014), and *Cyclotella petenensis* following Paillès et al. (2018).

The age-depth model for core C is based on seven AMS radiocarbon dated terrestrial samples and stratigraphical correlation with core A (Fleury et al., 2014). We used a linear regression between the available radiocarbon dated samples (Fig. A7) which is comparable with the age-depth model of Fleury et al. (2014) for the time window between ~2500 BCE and 1000 CE.

Wavelet transfer functions

The relation between our beach ridge and diatom record and other palaeo-precipitation records from the Maya Lowlands and nearby regions (figure A1 and A2) were investigated by wavelet coherence (CWT) analyses using the software developed by Grinsted et al. (2004). We also applied CWT to compare our record with North Atlantic ice drift record (Bond et al., 2001) and the Northern Hemispheric atmospheric $\delta^{14}C$ record (Reimer et al., 2013) to gain an understanding of the forcing of the regional changes in precipitation we observe. The record of drift ice from the North Atlantic is bimodally distributed, oscillating between periods of low and high concentrations of hematite-stained grains. The timeseries was therefore transformed into a record of percentiles based on its cumulative distribution function to avoid leakage of the square wave into frequency bands outside the fundamental period (Grinsted et al., 2004). CWT applies Monte Carlo methods to test for significance. In this case we set the alpha value at 5%. Time periods and periodicities enclosed within the black lines of in our wavelet analysis indicate common power between timeseries with 95% confidence.

3. Results

Beach-ridge record

As described above, when beach ridge elevation is largely driven by the discharge of the Usumacinta River, periods of relative high (low) beach ridges correspond to relatively drier (wetter) conditions in the Usumacinta catchment (Fig. 2). The beach-ridge record shows clear centennial scale variability, with an exceptionally dry phase centred around 1000 ± 95 BCE, and a subsequent pronounced wet phase centred around 800 ± 95 BCE.

Diatom record Lake Tuspan

The sediment stratigraphy of core C can be divided into two main units. Below 4.3 m the core is clearly laminated, and 0.5-4-cm-thick dark palaeoflood-layers contrast with the predominantly light-coloured calcareous deposits. The flood-layers are characterized by elevated detrital input, resulting in elevated concentrations of Si, amorphous silica, and charred plant fragments. The average recurrence time of large floods was approximately 50 years. Sediments from 0.25 to 4.3 m depth are vaguely laminated, with three distinct dm-thick turbidite layers (Fig. 3).

The interpretation of PC-1 (Fig. 3) as an indicator of lake salinity and hence relative dryness (see Methods) is supported by the fact that low/negative PC-1 values are driven by relatively high percentages of *Plagiotropis arizonica* (Fig. 3), a diatom species characteristic of high-conductivity water bodies (Czarnecki and Blinn, 1978) as well as other benthic, high salinity/alkalinity species such as *Anomoeoneis sphaerophora* and *Craticula cuspidata* (Fig. A4).

A drastic change from dry to wet conditions occurred around 4.3 m depth (¬1100 BCE), with the loss of salinity tolerant taxa and higher proportions of freshwater taxa such as *Eunotia* sp. and *Cyclotella petenensis* (Fig. 3). This coincides with the observed lithological shift from clearly to vaguely laminated sediments. After relatively high/positive PC-1 values during the Middle and Late Pre-Classic Period we observe a decreasing trend in PC-1 values during the following Classic Period, indicating a gradual increase in lake water salinity. Low PC-1 values between 800 – 950 CE are in accordance with many palaeorecords from the area (Fig. A2) indicating periods of prolonged droughts during the Late Classic Period.

Wavelet transfer function

Wavelet coherence (WTC) analysis (Grinsted et al., 2004) indicates in-phase coherence between the beach ridge record and the recently extended and revised calcite $\delta^{18}O$ speleothem record from Macal-Chasm cave (Akers et al., 2016) (Fig. A7). The in-phase relationship between the two records is significant above a 5% confidence level at centennial timescales during the Pre-Classic Period. We did not find significant relationships between the beach ridge record and other palaeo-precipitation records from the CML, nor with records from the Yucatan and Central Mexico (Fig. A2), except for a significant in-phase coherence at a centennial time scale with the *Pyrgophorus* sp. $\delta^{18}O$ record from Lake Chichancanab (Hodell et al., 1995).

4. Discussion

4.1 Climate change in the CML during the Pre-Classic period

Early Pre-Classic period (1800 – 1000 BCE)
Both beach ridge and diatom records indicate that the onset of the early Pre-Classic period was relatively dry (Fig. 4). Despite the predominantly dry conditions, large floods still occurred, as demonstrated by the repetitive input of fluvial material into Lake Tuspan. Periods with the highest fluvial sediment input coincided with periods of increased input of charcoal into Lake Peten-Itza (Schüpbach et al., 2015) (Fig. A2). Because the CML were still sparsely populated during the Early Pre-Classic period (Inomata et al., 2015) we relate the presence of charcoal to the occurrence of wildfires.

After a transition to wetter conditions between 1500 and 1400 BCE, we observe a drying trend that culminated in a prolonged dry period at the end of the Early Pre-Classic period centred around 1000 ± 95 BCE. Although this exceptionally dry phase is less apparent from Lake Tuspan's diatom record (Fig. 3), it has been recorded at many other sites within the CML. At Lake Puerto Arturo, high $\delta^{18}O$ values in the gastropod *Pyrgophorus* sp. indicate that this was the driest period since 6300 BCE (Wahl et al., 2014), and the recently extended and improved speleothem $\delta^{18}O$ record from Macal Chasm indicates that this dry period was probably at least as severe as any prolonged droughts during the Classic and Post-Classic period (Akers et al., 2016). Dry conditions are reflected in high $Ca/\Sigma(Ti,Fe,Al)$ values at Lake Peten-Itza (Mueller et al., 2009), indicating elevated authigenic carbonate ($CaCO_3$) precipitation relative to the input of fluvial detrital elements (Ti, Fe and Al) during this period; water level at this large lake must have dropped by at least 7 m (Mueller et al., 2009).

Middle Pre-Classic period (1000 – 400 BCE)
Both the beach ridge and the Lake Tuspan diatom records indicate a change to wetter conditions around 1000-850 BCE, causing major changes in hydrological conditions in the CML (Fig. 4). The diatom assemblages in the Lake Tuspan record show a major change in composition. Species indicative of meso- to polysaline water almost completely disappear, and are replaced by species indicating fresh water conditions (Fig. 4). In the lake sediments, this transition is also marked by a lithological shift from clearly to vaguely laminated sediments that lack repetitive large flood layers, while charred plant fragments are almost absent until ~400 BCE. Similar abrupt lithological transitions were reported from Lake Chichancanab (Hodell et al., 1995) and Lake Peten-Itza (Mueller et al., 2009), and Wahl et al. (2014) describe a regime shift at Puerto Arturo. The sudden reduction in charred plant fragments around ~1000 BCE at Lake Tuspan coincides with reduced concentrations of charcoal at Lake Peten-Itza (Fig. A2) (Schupbach et al., 2015) and Laguna Tortuguero, Puerto Rico (Burney and Pigott Burney, 1994) indicating rapid climatic changes over a large spatial scale.

Late Pre-Classic period (400 BCE – 250 CE)
Both beach ridge and diatom record (Fig. 4) indicate that a relatively dry period occurred by the onset of the Late Pre-Classic period, which has not been identified in other proxy records from the region (Fig. A2), although high *Pinus* pollen percentages in the pollen record from Petapilla pond near Copan (McNeil, 2010) during this period may indicate dry conditions, as high *Pinus* pollen percentage at highland sites could be indicative of drier conditions (Domínguez-Vázquez and Islebe, 2008). The diatom record at Lake Tuspan (Fig. 3) shows a general increase in lake water salinity, indicating a gradual shift to drier conditions in the Late Pre-Classic period.

4.2 Precipitation variability

Precipitation variability over long time scales
The observed general drying trend over the last few thousand years is probably related to the southward shift of the ITCZ during the late Holocene. The shift occurred in response to orbitally-forced changes in insolation (Haug et al., 2001), causing a gradual Northern Hemisphere cooling versus Southern Hemisphere warming (Fig. 4), thereby shifting the ITCZ towards the warming southern hemisphere (Schneider et al., 2014). Wetter conditions during the Middle Pre-Classic period may reflect a more northerly position of the ITCZ, which may be related to stronger easterly tradewinds and the less frequent occurrence of winter season cold fronts, as beach ridge morphological changes suggest (Nooren et al., 2017b).

Centennial-scale precipitation variability
The coherence between the beach ridge record and the relatively well-dated Macal-Chasm speleothem record gives us confidence that these records reflect regionally coherent variability at centennial timescales during the Pre-Classic period. Interestingly, the beach ridge record is significantly in anti-

phase with the North Atlantic ice drift record (Bond et al., 2001) and the Northern Hemispheric atmospheric $\delta^{14}C$ record during the Pre-Classic Period (Reimer et al., 2013) (Fig. 5), suggesting an important role of North Atlantic atmospheric-oceanic forcing on precipitation in the CML. The Northern Hemispheric atmospheric $\delta^{14}C$ record shows a 512-yr periodicity (Stuiver and Braziunas, 1993), which is similar to the observed ~500 year periodicity of the beach ridge record during the Pre-Classic period. Such a centennial scale periodicity is not apparent in Lake Tuspan's diatom record (Fig. 3), nor in any of the other palaeo-precipitation records from the Maya Lowlands (Fig. A2), but has been identified in the Ti record from Lake Juanacatlán in the highlands of Central Mexico (Jones et al., 2015). This periodicity has been related to the intensity of the North Atlantic thermohaline circulation and variations in solar activity (Stuiver and Braziunas, 1993).

The coherence with fluctuations in solar irradiance is most evident during the 850 BCE (2.8 ka) event, related to the Homeric Grand Solar Minimum. At that time, a strong decrease in the total solar irradiance resulted in higher atmospheric ^{14}C production and a change to cooler and wetter conditions in the Northern Hemisphere (e.g. Van Geel et al., 1996), and apparently also a shift to wetter conditions in the CML, evident from our two new palaeo-precipitation records (Fig. 4). This correlation should not be used as an analogue for modern precipitation variability, when periods of lower solar activity are associated with lower Usumacinta River discharge and hence less precipitation in the CML (Fig. A8). Probably due a more northerly mean position of the ITCZ during the Pre-Classic Period precipitation responded differently to solar forcing then today.

It has previously been suggested that there was a coherent response to the late Holocene southward shift of the ITCZ in both northern South America and the Maya Lowlands (Haug et al., 2003), implying that the beach ridge record should be in-phase with the Cariaco Ti record (Haug et al., 2001). Although the Cariaco record indicates large centennial-scale variability in precipitation over northern South America (Fig. 4), this variability is not significantly correlated with the beach-ridge record. The correlation improved slightly using an updated age-depth model for Cariaco (Fig. A9), but remains insignificant, probably as a consequence of uncertainties in the chronological control of both records or because of a more prominent influence of the Northern Atlantic climatic forcing mechanisms in the Maya Lowlands.

4.3 Precipitation versus human development in the CML

Our records indicate that the Early Pre-Classic period in the CML was relatively dry. During that period, the CML were still sparsely populated by moving hunter-gatherers. It is highly likely that before maize became sufficiently productive to sustain sedentism, the karstic lowlands were less attractive for humans than the coastal wetlands along the Gulf of Mexico and Pacific coast, where natural resources were abundantly present to successfully sustain a hunting/gathering subsistence system (Inomata et al., 2015). Reliance on cultivated crops, most notably maize, rapidly increased after the onset of the Middle Pre-Classic period around 1000 BCE (Rosenswig et al., 2015). Between 1000 and 850 BCE, under still dry conditions, there is evidence for increased maize agriculture in the Pacific flood basin (Rosenswig et al., 2015), and within the Olmec area on the Gulf of Mexico coast (Arnold III, 2009), and maize grains (AMS ^{14}C dated to 875 ± 29 BCE) have been found as far as Ceibal within the CML (Inomata et al., 2015). We speculate that wetter conditions after 850 BCE might have been unfavourable for further development of intensive agriculture in the CML. This is supported by palynological evidence, indicating that widespread land clearance and agriculture activity did not occur before ~400 BCE (Wahl et al., 2007; Galop et al., 2004; Islebe et al., 1996; Leyden et al., 1987), despite some early local agricultural activity (Wahl et al., 2014; Rushton et al., 2013; McNeil et al., 2010). A return to drier conditions during the Late Pre-Classic period coincided with an expansion of maize-based agriculture in the CML, and communities within the Maya Lowlands show strong and steady development (Hansen, 2017; Inomata and Henderson, 2016). Hence, major development of Maya civilization in the Central Maya Lowlands occurred only after the onset of the Late Pre-Classic period, when climate became progressively drier, in line with earlier findings that drier conditions were favourable for agricultural development in the CML (Wahl et al., 2014). Changes in the distribution of rainfall probably also changed, and large floods, most evident during the Archaic and early Pre-Classic period, occurred much less frequently after approximately 1000 BCE.

5. Conclusions

For the first time a regional palaeo-precipitation record has been reconstructed for the Central Maya Lowland (CML), based on an exceptionally well dated high resolution beach ridge record. This record indicates centennial scale precipitation fluctuations during the Pre-Classic period that are not always registered in local records, adding valuable new insights into larger scale climatic forcing mechanisms for the CML. The generally poor correlation between the regional and local palaeo-precipitation reconstructions are probably related to spatial precipitation variability, and chronological uncertainties of many records. Additional research of beach ridge formation processes are needed to extend this regional precipitation reconstruction to the Classic and Post-Classic period.

We have also generated a local scale palaeo-precipitation record using diatoms preserved in a core from Lake Tuspan, thereby adding an alternative proxy to the relatively high number of local reconstructions predominantly based on oxygen isotope variability. We recognise, however, that diatom preservation is often poor in the carbonate lakes across the wider region. As a result, the correlation between these two reconstructions is variable through time.

Although the occurrence of a prolonged drought during the end of the Early Pre-Classic period, which we report here, is evident in other palaeo-precipitation reconstructions from the CML, the subsequent wet period during the Middle Pre-Classic period, registered in both our new records, is less evident elsewhere. Although many researchers have focused on the impact of drought on the development and disintegration of Maya societies, one should consider this prolonged wet period as potentially unfavourable for the development and intensification of agriculture in the CML, particularly in the wetter areas.

Our results provide evidence that North Atlantic atmospheric-oceanic forcing plays an important role in the modulation of the observed centennial scale precipitation variability, however further studies are required which compare well-dated terrestrial reconstructions that capture regional signals with solar and oceanic reconstructions to gain a better understanding of climate forcing mechanisms, both in the CML and across the wider region.

Acknowledgements

This research is supported by the Netherlands Organization for Scientific Research (NWO-grant 821.01.007). The LiDAR data was generously provided by INEGI, Mexico. We acknowledge Philippe Martinez, Jacques Giraudeau and Pierre Carbonel for the XRF core scan measurements, and we would like to thank Peter Douglas, Pete Akers and Gerald Haug for providing their data. We thank Konrad Hughen for valuable suggestions to update the age-depth model for Cariaco's sediment core 1002D. We thank Ton Markus for improving the figures, and Mark Brenner and an anonymous reviewer for their valuable comments to improve the paper.

References

Akers, P.D., Brook, G.A., Railsback, L.B., Liang, F., Iannone, G., Webster, J.W., Reeder, P.P., Cheng, H., and Edwards, R.L., An extended and higher-resolution record of climate and land use from stalagmite MC01 from Macal Chasm, Belize, revealing connections between major dry events, overall climate variability, and Maya sociopolitical changes. Palaeogr Palaeoclimatol Palaeoecol 459: 268-288, 2016.

Amador, J.A., Alfaro, E.J., Lizano, O.G., and Magaña, V.O., Atmospheric forcing of the eastern tropical Pacific: A review. Progress in Oceanography 69: 101-142, 2006.

Anselmetti, F.S., Hodell, D.A., Ariztegui, D., Brenner, M., and Rosenmeier, M.F., Quantification of soil erosion rates related to ancient Maya deforestation. Geology 35: 915–918, 2007.

Arnold III, P.J., Settlement and subsistence among the Early Formative Gulf Olmec. J Anthropol Archaeol 28: 397-411, 2009.

Banco Nacional de Datos de Aguas Superficiales, Conagua. http://www.conagua.gob.mx/CONAGUA07/Contenido/Documentos/Portada BANDAS.htm conagua.gob.mx/Bandas/Bases_Datos_Presas/, consulted January 2017.

Bhattacharya, T., Byrne, R., Böhnel, H., Wogau, K., Kienel, U., Ingram, B.L., and Zimmerman, S., Cultural implications of late Holocene climate change in the Cuenca Oriental, Mexico. Proc Natl Acad Sci USA 112(6), 1693–1698, 2015.

Batterbee, R.W., A new method for estimating absolute microfossil numbers with special reference to diatoms. Limnol Oceonogr 18: 647-653, 1973.

Beach, T., Luzzadder-Beach, S., Cook, D., Dunning, N., Kennett, D.J., Krause, S., Terry, R., Trein, D., and Valdez, F., Ancient Maya impacts on the Earth's surface: An Early Anthropocene analog? Quat Sci Rev 124: 1-30, 2015.

Bernal, J.P., Lachniet, M., McCulloch, M., Mortimer, G., Morales, P., and Cienfuegos, E., A speleothem record of Holocene climate variability from southwestern Mexico. Quat Res 75:104–113, 2011.

Bond, G., Kromer, B., Beer, J., Muscheler, R., Evans, M.N., Showers, W., Hoffmann, S., Lotti-Bond, R., Hajdas, I., and Bonani, G., Persistent Solar Influence on North Atlantic Climate During the Holocene. Science 294: 2130-2136, 2001.

Bronk Ramsey, C., Oxcal 4.2.; http://c14.arch.ox.ac.uk/oxcal.html, 2016.

Bronk Ramsey, C., Bayesian analysis of radiocarbon dates. Radiocarbon 51: 337–360, 2009.

Burney, D.A., and Pigott Burney, L., Holocene Charcoal Stratigraphy from Laguna Tortuguero, Puerto Rico, and the Timing of Human Arrival on the Island. J Archaeol Sci 21: 273-281, 1994.

Coe, M.D., The Maya, eight edition, Thames and Hudson, London, UK, 2011.

Curtis, J.H., and Hodell, D.A., Climate Variability on the Yucatan Peninsula (Mexico) during the Past 3500 Years, and Implications for Maya Cultural Evolution. Quat Res 46: 37-47, 1996.

Curtis, J.H., Brenner, M., Hodell, D.A., Balser, R.A., Islebe, G.A., and Hooghiemstra, H., A multiproxy study of Holocene environmental change in the Maya Lowlands of Peten, Guatemala. J Paleolimnol 19: 139–159, 1998.

Czarnecki, D.B., and Blinn, D.W., Observations on Southwestern Diatoms. I. Plagiotropis arizonica N. Sp. (Bacillariophyta, Entomoneidaceae), a large Mesohalobous Diatom. Trans Am Microsc Soc 97: 393-396, 1978.

Davies, S. J., Lamb, H. F., & Roberts, S. J. Micro-XRF Core Scanning in Palaeolimnology: Recent Developments. In Croudace and Rothwell (eds) *Micro-XRF Studies of Sediment Cores*, Springer. pp. 189-226, 2015.

Dermody, B.J., van Beek, R.P.H., Meeks, E., Klein Goldewijk, K., Scheidel, W., van der Velde, Y., Bierkens, M.F.P., Wassen, M.J., Dekker, S.C., A virtual water network of the Roman world. Hydrol. Earth Syst. Sci. 18, 5025–5040, 2014.

Díaz, K.A., Pérez, L., Correa-Metrio, A., Franco-Gaviria, J.F., Echeverria, P., Curtis, J., and Brenner, M., Holocene environmental history of tropical, mid-altitude Lake Ocotalito, México, inferred from ostracodes and non-biological indicators. Holocene 27, 1308-1317, 2017.

Domínguez-Vázquez, G., and Islebe, G.A., Protracted drought during the late Holocene in the Lacandon rain forest, Mexico. Veg Hist Archaeobot 17: 327-333, 2008.

Douglas, P.M.J., Demarest, A.A., Brenner, M., and Canuto, M.A., Impacts of Climate Change on the Collapse of Lowland Maya Civilization. Annu Rev Earth Planet Sci 44: 613–645, 2016.

Douglas, P.M.J., Pagani, M., Canuto, M.A., Brenner, M., Hodell, D.A., Eglinton, T.I., and Curtis, J.H., Drought, agricultural adaptation, and sociopolitical collapse in the Maya Lowlands. Proc Natl Acad Sci USA 112: 5607-5612, 2015.

Dunning, N.P., Beach, T.P., and Luzzadder-Beach, S., Kax and kol: Collapse and resilience in lowland Maya civilization. Proc Natl Acad Sci USA 109(10): 3652–3657, 2012.

Dunning, N.P., McCane, C., Swinney, T., Purtill, M., Sparks, J., Mann, A., McCool, J.-P., and Ivenso, C., Geoarchaeological Investigations in Mesoamerica Move into the 21st Century: A Review. Geoarchaeology 30: 167–199, 2015.

Ebert, C.E., Peniche May, N., Culleton, B.J., Awe, J.J., and Kennett, D.J., Regional response to drought during the formation and decline of PreClassic Maya societies. Quat Sci Rev 173, 211-235, 2017.

Fleury, S., Malaizé, B., Giraudeau, J., Galop, D., Bout-Roumazeilles, V., Martinez, P., Charlier, K., Carbonel, P., and Arnauld, M.-C., Impacts of Mayan land use on Laguna Tuspan watershed (Petén, Guatemala) as seen through clay and ostracode analysis. J Archaeol Sci 49: 372–382, 2014.

Ford, A., and Nigh, R., The Maya Forest Garden: Eight Millennia of Sustainable Cultivation of the Tropical Woodland, Taylor and Francis, London, New York, 2015.

Galop, D., Lemonnier, E., Carozza, J.M., and Metailie, J.P., Bosques, milpas, casas y aguadas de antaño. In: La Joyanca, ciudad maya del noroeste del Peten (Guatemala), Arnauld C. et Breuil-Martinez V. (eds.). CEMCA, CIRMA, Associacion Tikal, Guatemala, 55-71, 2004.

Gasse, F., Juggins, S., and Ben Khelifa, L., Diatom-based transfer functions for inferring past hydrochemical characteristics of African lakes. Palaeogeogr Palaeoclimatol Palaeoecol 117: 31-54, 1995.

Grinsted, A., Moore, J.C., and Jevrejeva, S., Application of the cross wavelet transform and wavelet coherence to geophysical time series. Nonlinear Processes Geophys 11: 561-566, 2004.

Hansen, R.D., The Feast Before Famine and Fighting: The Origins and Consequences of Social Complexity in the Mirador Basin, Guatemala. Feast, Famine or Fighting? Multiple Pathways to Social Complexity, Chacon, R.J., and Mendoza, R.G. (eds), Springer, Dordrecht, the Netherlands, pp 305-335, 2017.

Haug, G.H., Hughen, K.A., Sigman, D.M., Peterson, L.C., and Röhl, U., Southward Migration of the Intertropical Convergence Zone Through the Holocene. Science 293, 1304–1308, 2001.

Haug, G.H., Gunther, D., Peterson, L.C., Sigman, D.M., Hughen, K.A., and Aeschlimann, B., Climate and the Collapse of Maya Civilization. Science 299: 1731-1735, 2003.

Hijmans, R.J., Cameron, S.E., Parra, J.L., Jones, P.G., and Jarvis, A., Very high resolution interpolated climate surfaces for global land areas. Int J of Clim 25: 1965-1978, 2005.

Hodell, D.A., Brenner, M., and Curtis, J.H., Climate and cultural history of the Northeastern Yucatan Peninsula, Quintana Roo, Mexico. Climatic Change 83: 215–240, 2007.

Hodell D.A., Brenner, M., and Curtis, J.H., Terminal Classic drought in the northern Maya lowlands inferred from multiple sediment cores in Lake Chichancanab (Mexico). Quat Sci Rev 24: 1413–1427, 2005.

Hodell, D.A., Brenner, M., Curtis, J.H., and Guilderson, T., Solar forcing of drought frequency in the Maya lowlands. Science 292: 1367–1369, 2001.

Hodell, D.A., Curtis, J.H., and Brenner, M., Possible role of climate in the collapse of Classic Maya civilization. Nature 375: 391–394, 1995.

Hoggarth, J.A., Breitenbach, S.F.M., Culleton, B.J., Ebert, C.E., Mason, M.A., and Kennett, D.J., The political collapse of Chichén Itzá in climatic and cultural context. Glob Planet Change 138: 25-42, 2016.

Iannone, G., The Great Maya Droughts in Cultural Context: Case Studies in Resilience and Vulnerability, Univ Press of Colorado, Boulder, CO, USA, 2014.

Inomata, T., and Henderson, L., Time tested: re-thinking chronology and sculptural traditions in Preclassic southern Mesoamerica. Antiquity 90: 456-471, 2016.

Inomata, T., MacLellan, J., Triadan, D., Munson, J., Burham, M., Aoyama, K., Nasu, H., Pinzón, F., and Yonenobu, H., Development of sedentary communities in the Maya lowlands: Coexisting mobile groups and public ceremonies at Ceibal, Guatemala. Proc Natl Acad Sci USA 112: 4268–4273, 2015.

Islebe, G.A., Hooghiemstra, H., Brenner, M., Curtis, J.H., and Hodell, D.A., A Holocene vegetation history from lowland Guatemala. Holocene 6: 265–271, 1996.

Jones, M.D., Metcalfe, S.E., Davies, S.J., and Noren, A., Late Holocene climate reorganisation and the North American Monsoon. Quat Sci Rev 124: 290-295, 2015.

Kalnay E., Kanamitsu, M., Kistler, R., Collins, W., Deaven, D., Gandin, L., Iredell, M., Saha, S., White, G., Woollen, J., Zhu, Y., Chelliah, M., Ebisuzaki, W., Higgins, W., Janowiak, J., Mo, K.C., Ropelewski, C., Wang, J., Leetmaa, A., Reynolds, R., Jenne, R., and Joseph, D., The NCEP/NCAR Reanalysis 40-year Project. Bull Am Meteorol Soc 77: 437–471, 1996.

Kennett, D.J., Breitenbach, S.F.M., Aquino, V.V., Asmerom, Y., Awe, J., Baldini, J.U.L., Bartlein, P., Culleton, B.J., Ebert, C., Jazwa, C., Macri, M.J., Marwan, N., Polyak, V., Prufer, K.M., Ridley, H.E., Sodemann, H., Winterhalder, B., and Haug, G.H., Development and disintegration of Maya political systems in response to climate change. Science 338: 788–791, 2012.

Kopp, G., and Lean, J.L., A new, lower value of total solar irradiance: Evidence and climate significance. Geophys Res Lett 38: L01706, 2011.

Krivova, N.A., Balmaceda, L., and Solanki, S.K., Reconstruction of solar total irradiance since 1700 from the surface magnetic flux. Astron Astrophys 467: 335–346, 2007.

Lachniet, M.S., Asmerom, Y., Bernal, J.P., Polyak, V., and Vazquez-Selem, L., Orbital pacing and ocean circulation-induced collapses of the Mesoamerican monsoon over the past 22,000 y. Proc Natl Acad Sci USA 110: 9255–9260, 2013.

Lachniet, M.S., Asmerom, Y., Polyak, V., and Bernal, J.P., Two millennia of Mesoamerican monsoon variability driven by Pacific and Atlantic synergistic forcing. Quat Sci Rev 155: 100-113, 2017.

Lee, S., Gaiser, E., VanDeVijver, B., Edlund, M.B., and Spaulding, S.A., Morphology and typification of *Mastogloia smithii* and *M. lacustris*, with descriptions of two new species form the Florida Everglades and the Caribbean region. Diatom research 29: 325-350, 2014.

Lentz, D.L., Dunning, N.P., Scarborough, V.L., Magee, K.S., Thompson, K.M., Weaver, E., Carr, C., Terry, R.E., Islebe, G., Tankersley, K.B., Grazioso Sierra, L., Jones, J.G., Buttles, P., Valdez, F., and Ramos Hernandez, C.E., Forests, fields, and the edge of sustainability at the ancient Maya city of Tikal. Proc Natl Acad Sci USA 111: 18513–18518, 2014.

Leyden. B.W., Man and Climate in the Maya Lowlands. Quat Res 28: 407-414, 1987.

Lohse, J., Archaic Origins of the Lowland Maya. Latin American Antiquity 21: 312-352, 2010.

McNeil, C.L., Burney, D.A., and Burney, L.P., Evidence disputing deforestation as the cause for the collapse of the ancient Maya polity of Copan, Honduras. Proc Natl Acad Sci USA 107: 1017–1022, 2010.

Medina-Elizalde, M., Burns, S.J., Polanco-Martinez, J.M., Beach, T., Lases-Hernandez, F., Shen, C.C., and Wang, H.C., High-resolution speleothem record of precipitation from the Yucatan Peninsula spanning the Maya Preclassic Period. Glob Planet Change 138: 93-102, 2016.

Medina-Elizalde, M., Burns, S.J., Lea, D.W., Asmerom, Y., von Gunten, L., Polyak, V., Vuille, M., and Karmalkar, A., High resolution stalagmite climate record from the Yucatan Peninsula spanning the Maya terminal classic period. Earth Planet Sci Lett 298: 255–262, 2010.

Metcalfe, S.E., Barron, J.A., and Davies, S.J., The Holocene history of the North American Monsoon: ‘known knowns’ and ‘known unknowns’ in understanding its spatial and temporal complexity. Quat Sci Rev 120: 1-27, 2015.

Metcalfe, S., Breen, A., Murray, M., Furley, P., Fallick, A., and McKenzie, A., Environmental change in northern Belize since the latest Pleistocene. J Quat Sci 24: 627-641, 2009.

Mueller, A.D., Islebe, G.A., Hillesheim, M.B., Grzesik, D.A., Anselmetti, F.S., Ariztegui, D., Brenner, M., Curtis, J.H., Hodell, D.A., and Venz, K.A., Climate drying and associated forest decline in the lowlands of northern Guatemala during the Holocene. Quat Res 71: 133-141, 2009.

Nooren, K., Hoek, W.Z., Van der Plicht, H., Sigl, M., Van Bergen, M.J., Galop, D., Torrescano-Valle, N., Islebe, G., Huizinga, A., Winkels, T., and Middelkoop, H., Explosive eruption of El Chichón volcano (Mexico) disrupted 6th century Maya civilization and contributed to global cooling. Geology 45: 175-178, 2017a.

Nooren, K., Hoek, W.Z., Winkels, T., Huizinga, A., Van der Plicht, H., Van Dam, R.L., Van Heteren, S., Van Bergen, M.J., Prins, M.A., Reimann, T., Wallinga, J., Cohen, K.M., Minderhoud, P., and Middelkoop, H., The Usumacinta-Grijalva beach-ridge plain in southern Mexico: a high-resolution archive of river discharge and precipitation. Earth Surf Dynam 5: 529-556, 2017b.

Novelo, E., Tavera, R., and Ibarra, C., Bacillariophyceae from karstic wetlands in Mexico, J. Cramer, Berlin, Germany, 2007.

Paillès, C., Sylvestre, F., Escobar, J., Tonetto, A., Rustig, S., and Mazur, J-C, *Cyclotella petenensis* and *Cyclotella cassandrae*, two new fossil diatoms from Pleistocene sediments of Lake Petén-Itzá, Guatemala, Central America. Phytotaxa 351: 247-263, 2018.

Patrick, R., and Reimer, C.W., Diatoms of the United States, Vol. I, Monograph 13, Acad Nat Sci, Philadelphia, USA, 1966.

Patrick, R., Reimer, C.W., Diatoms of the United States, Vol. II, Part1, Monograph 13, Acad Nat Sci, Philadelphia, USA. 1975.

Pollock, A.L., Van Beynen, P.E., De Long, K.L., Polyak, V., Asmerom, Y., and Reeder, P.P., A mid-Holocene paleoprecipitation record from Belize. Palaeogeogr Palaeoclimatol Palaeoecol 463: 103-111, 2016.

Reed, J.M., A diatom-conductivity transfer function for Spanish salt lakes. J Paleolimnol 19: 399-416, 1998.

Reimer, P.J., Bard, E., Bayliss, A., Warren Beck, J., Blackwell, P.G., Ramsey, C.B., Buck, C.E., Cheng, H., Lawrence Edwards, R., Friedrich, M., Grootes, P.M., Guilderson, T.P., Haflidason, H., Hajdas, I., Hatté, C., Heaton, T.J., Hoffmann, D.L., Hogg, A.G., Hughen, K.A., Felix Kaiser, K., Kromer, B., Manning, S.W., Niu, M., Reimer, R.W., Richards, D.A., Marian Scott, E., Southon, J.R., Staff, R.A, Turney, C.S.M., and Van der Plicht, J., IntCal13 and Marine13 radiocarbon age calibration curves 0–50,000 years cal BP. Radiocarbon 55: 1869–1887, 2013.

Rosenmeier, M.F., Hodell, D.A., Brenner, M., Curtis, J.H., and Guilderson, T.P., A 4000-year lacustrine record of environmental change in the southern Maya lowlands, Peten, Guatemala. Quat Res 57: 183–190, 2002.

Rosenswig, R.M., VanDerWarker, A.M., Culleton, B.J., and Kennett, D.J., Is it agriculture yet? Intensified maize-use at 1000 cal BC. in the Soconusco and Mesoamerica. J Antropol Archaeol 40: 89-108, 2015.

Rushton, E.A.C., Metcalfe, S.E., and Whitney, B.S.W., A late-Holocene vegetation history from the Maya Lowlands, Lamanai, Northern Belize. Holocene 23: 485-493, 2013.

Schneider, T., Bischoff, T., and Haug, G.H., Migrations and dynamics of the intertropical convergence zone. Nature 513: 45-53, 2014.

Schüpbach, S., Kirchgeorg, T., Colombaroli, D., Beffa, G., Radaelli, M., Kehrwald, N.M., and Barbante, C., Combining charcoal sediment and molecular markers to infer a Holocene fire history in the Maya Lowlands of Petén, Guatemala. Quat Sci Rev 115: 123-131, 2015.

Steinhilber, F. Abreu, J.A., Beer, J., Brunner, I., Christl, M., Fischer, H., Heikkilä, U., Kubik, P.W., Mann, M., McCracken, K.G., Miller, H., Miyahara, H., Oerter, H., and Wilhelms, F., 9,400 years of cosmic radiation and solar activity from ice cores and tree rings. Proc Natl Acad Sci USA 109: 5967–5971, 2012.

Stuiver, M., and Braziunas, T.F., Sun, ocean, climate and atmospheric $^{14}CO_2$: an evaluation of causal and spectral relationships. Holocene 3: 289-305, 1993.

Tankersley, K.B., Dunning, N.P., Scarborough, V., Huff, W.D., Lentz, D.L., and Carr, C., Catastrophic volcanism and its implication for agriculture in the Maya Lowlands: J Archaeol Sci 5, 465–470, 2016.

Thompson, J.E.S., A Commentary on the Dresden Codex, Am Philosophical Society, Philadelphia, USA, 1972.

Torrescano-Valle, N., and Islebe, G.A., Holocene paleoecology, climate history and human influence in the southwestern Yucatan Peninsula. Rev Palaeobot Palynol 217: 1-8, 2015.

Turner II, B.L., and Sabloff, J.A., Classic Period collapse of the Central Maya Lowlands: Insights about human-environment relationships for sustainability. Proc Natl Acad Sci USA 109: 13908–13914, 2012.

USGS, Shuttle Radar Topography Mission (SRTM) 1 Arc-Second Global dataset. https://lta.cr.usgs.gov/SRTM1Arc, 2009.

Valásquez Garciá, E., The Maya Flood Myth and the Decapitation of the Cosmic Caiman. The PARI Journal 7: 1-10, 2006.

Van Geel, B., Buurman, J., and Waterbolk, H.T., Archaeological and palaeoecological indications for an abrupt climate change in The Netherlands and evidence for climatological teleconnections around 2650 BP. J Quat Sci 11: 451–460, 1996.

Velez, M.I., Curtis, J.H., Brenner, M., Escobar, J., Leyden, B.W., and Popenoe de Hatch, M., Environmental and Cultural Changes in Highland Guatemala Inferred from Lake Amatitlán Sediments. Geoarchaeology 26: 1-19, 2011.

Wahl, D., Byrne, R., and Anderson, L., An 8700 year paleoclimate reconstruction from the southern Maya lowlands. Quat Sci Rev 103: 19–25, 2014.

Wahl, D., Byrne, R., Schreiner, T., and Hansen, R., Palaeolimnological evidence of late-Holocene settlement and abandonment in the Mirador Basin, Peten, Guatemala. Holocene 17: 813-820, 2007.

Figure captions

Figure 1: The image on page 74 of the Codex Dresden depicts a torrential downpour probably associated with a destructive flood (Thompson, 1972).

Figure 2: A large part of the Central Maya Lowlands (outlined with a red dashed line) is drained by the Usumacinta (Us.) River (A). During the Pre-Classic period this river was the main supplier of sand contributing to the formation of the extensive beach ridge plain at the Gulf of Mexico coast (B).

Periods of low rainfall result in low river discharges and are associated with relatively elevated beach ridges. The extent of the watersheds of the Usumacinta and Dulce River is calculated from SRTM 1-arc data (USGS, 2009). Indicated are archaeological sites (squares) and proxy records discussed in the text; Tu= Lake Tuspan, Ch = Lake Chichancanab, PI = Lake Peten-Itza, MC = Macal Chasm Cave, and PA = Lago Puerto Arturo.

Figure 3: Summarized proxy record of Lake Tuspan sediment core C. In the lithological column black lines represent large flood layers and grey boxes turbidites. Ca and Si (in cps = counts per second) are presented here as % of total counts. Vertical lines (red) in the (amorphous) Si graphs indicate the one-standard-deviation threshold above the mean. For the diatom record only the relative abundance of 'key' diatom species are shown here. *Denticula elegans* and *Nitzschia amphibia* were excluded from the diatom sum. Notice abrupt change around 1100 BCE.

Figure 4: Comparison of the Lake Tuspan and beach ridge record (A) with local and proximal records from Macal-Chasm cave (Akers et al., 2016) and the Cariaco basin (Haug et al., 2001)(B). We used an updated age-depth model for the Cariaco record (Fig. A9). Climate records related to North Atlantic atmospheric-oceanic forcing are indicated in panel C, including the drift ice reconstruction from the North Atlantic (Bond et al., 2001), the Northern Hemispheric residual atmospheric $\delta^{14}C$ content (Reimer et al., 2013), the Northern-to Southern hemispheric temperature anomaly (Schneider et al., 2014) and reconstructed Total Solar Irradiance (TSI) (Steinhilber et al., 2012).

Figure 5:Wavelet Transform Coherence (WTC) analysis between the beach ridge record and the Northern Hemispheric atmospheric $\delta^{14}C$ record (Reimer et al., 2013)(A) and the North Atlantic ice drift record (Bond et al., 2001)(B). The beach ridge record is significantly in anti-phase with both records at approximately 500-yr time scale, indicating an important role of North Atlantic atmospheric-oceanic forcing on precipitation in the Maya Lowlands during the Pre-Classic period. The 5% significance level against red noise is shown as a thick contour. Arrows indicate phase difference, with in-phase relationship between records if arrows point to the right.

Appendix: Additional figures

Figure A1: Location of proxy records indicated in figure A2 and/or mentioned in the main text. A: Northern Maya Lowlands (Tz=Tzabnah, PL=Punta Laguna, RS=Rio Secreto, Ch=Chichancanab and Si=Silvituc), the Central and Southern Maya Lowlands (PA=Puerto Arturo, NRL=New River Lagoon, Tu=Tuspan, PI/Sa=Peten-Itza and Salpeten, MC/CH=Macal Chasm and Chen Ha, and YB=Yok Balum), the Maya Highlands (Oc/Na= Ocotalito and Naja, Am=Amatitlan, and Pet=Petapilla). B: Central Mexico (Jua=Juanacatlan, CdD=Cueva de Diablo, Jx=Juxtlahuacan, and Alj=Aljojuca) and the marine record from the Cariaco (C) basin. Annual precipitation (1950-2000) calculated with WorldClim version 1.4 (release3); Hijmans et al. (2005). Long-term (1958-1998) mean ITCZ position and wind at 925 hPa ($m.s^{-1}$) for July after Amador et al. (2006), based on NCED/NCAR Reanalysis data (Kalnay et al., 1996).

Figure A2a: Palaeoprecipitation records from the Central Maya Lowlands and Yucatan; Beach ridge elevation and Tuspan diatom record (this study), compiled record of Central Peten and Yucatan (Douglas et al., 2016), Salpeten and Chichancanab dD wax-corr. (Douglas et al., 2015), Salpeten $\delta^{18}O$ (Rosenmeier et al., 2012), Peten-Itza $\delta^{18}O$ (Curtis et al., 1998), Puerto Arturo $\delta^{18}O$ (Wahl et al., 2014), Macal Chasm $\delta^{18}O$ (Akers et al., 2016), Chen Ha $\delta^{18}O$ (Pollock et al., 2016), Yok Balum $\delta^{18}O$ (Kennett et al., 2012), Rio Secreto $\delta^{18}O$ (Medina-Elizalde et al., 2016), Silvituc DV-pollen (Torrescano-Valle and Islebe, 2015), Chichancanab S and $\delta^{18}O$ (Hodell et al., 1995), Punta Laguna $\delta^{18}O$ (Hodell et al., 2007), and Tzabnah $\delta^{18}O$ (Medina-Elizalde et al., 2010). Notice that the y-axis is sometimes reversed, so that excursions above the x-axis always indicate relatively drier conditions.

Figure A2b: Proxy records from the Central Maya Lowlands, the Maya Highlands and Central Mexico. Peten-Itza charcoal (Schüpbach et al., 2015), Peten-Itza pollen (Islebe et al., 1996), Amatitlan *Aulacoseira* and *Pinus* (Velez et al., 2011), Petapilla *Pinus* (McNeil et al., 2010), Naja *Pinus* (Domínguez-Vázquez and Islebe, 2008), Ocotalito Sr (Díaz et al., 2017), Aljojuca $\delta^{18}O$ (Bhattacharya et al., 2015), Cueva del Diablo $\delta^{18}O$ (Bernal et al., 2011), Juxtlahuaca $\delta^{18}O$ (Lachniet et al., 2015, 2017), and Juanacatlan Ti 15-point running mean (Jones et al., 2015).

Figure A3: Age-distance model for beach ridge transect B. We refer to Nooren et al. (2017b) for further details.

Figure A4: Diatom record for lake Tuspan core C. Diatom concentrations (*1000 valves/g dw) were determined on 37 selected 1-cm samples and diatom percentages (only the ‘key species’ are shown here) were determined on the 123 subsamples at 4-12-cm contiguous intervals. The small and often dominant *Denticula elegans* and *Nitzschia amphibia* species were excluded from the diatom sum.

Figure A5: Detailed diatom record around one of the larger flood events ~1200 BCE.

Figure A6: Age-depth model for Tuspan core C. The age-depth model is based on a linear interpolation between calibrated ages of radiocarbon dated terrestrial macroremains from core A (Galop et al., 2004) and core C (Fleury et al., 2014). The model is most reliable for ages between ~2500 BCE and 1000 CE.

Figure A7: Wavelet Transform Coherence (WTC) analysis between the beach ridge record and the Macal Chasm $\delta^{18}O$ record (Akers et al., 2016). The 5% significance level against red noise is shown as a thick contour. Arrows indicate phase difference, with in-phase relationship between records if arrows point to the right.

Figure A8: Mean annual discharge of the Usumacinta river at Boca del Cerro (Banco Nacional de Datos de Aguas Superficiales, consulted in January 2017) compared with the total solar irradiance (TSI). The TSI is comprised of the reconstruction from 1700-2004 (Krivovo at al., 2007), concatenated with observations from the Total Irradiance Monitor (TIM) on NASA's Solar Radiation and Climate Experiment (SORCE) from 2005-2011 (Kopp and Lean, 2011). 4.56 watts are added to the TIM measurements as previous reconstructions were calibrated against less accurate measuring equipment, compared with the TIM instrument, which led to an overestimation of TSI.

Figure A9: Updated age-depth model for Cariaco core 1002D. Original model (Haug et al., 2001) has been based on a linear interpolation of calibrated ages. We applied a 4^{th}-order polynomal fit through modelled ages calculated with a P_sequence model (Oxcal 4.2) (Bronk Ramsey, 2009, 2016): k = 10, Marine13 calibration curve, delta R = 15 ± 50, one outlier: NSRL-13050.

Fig. 1

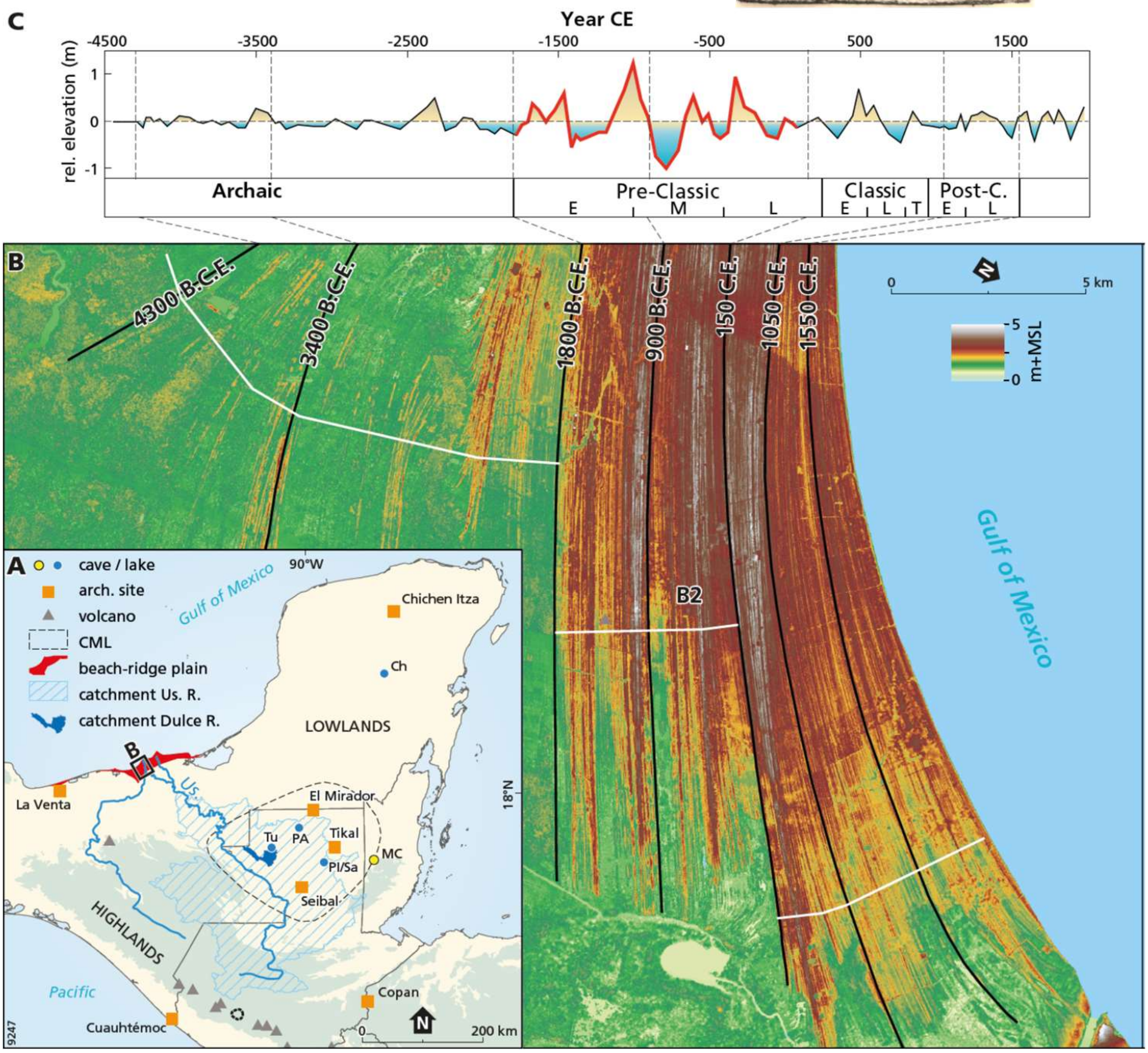

C
Year CE
-4500
-3500
-2500
-1500
-500
500
1500
rel. elevation (m)
1
0
-1
Archaic
Pre-Classic
E
M
L
Classic
E
L
T
Post-C.
E
L
B
4300 B.C.E.
3400 B.C.E.
1800 B.C.E.
900 B.C.E.
150 C.E.
1050 C.E.
1550 C.E.
0
5 km
5
0
m+MSL
B2
Gulf of Mexico
A
cave / lake
arch. site
volcano
CML
beach-ridge plain
catchment Us. R.
catchment Dulce R.
90°W
Gulf of Mexico
Chichen Itza
Ch
LOWLANDS
B
La Venta
Us.
El Mirador
Tu
PA
Tikal
Pl/Sa
MC
Seibal
18°N
HIGHLANDS
Pacific
Copan
Cuauhtémoc
0
200 km
N
9247

Fig. 2

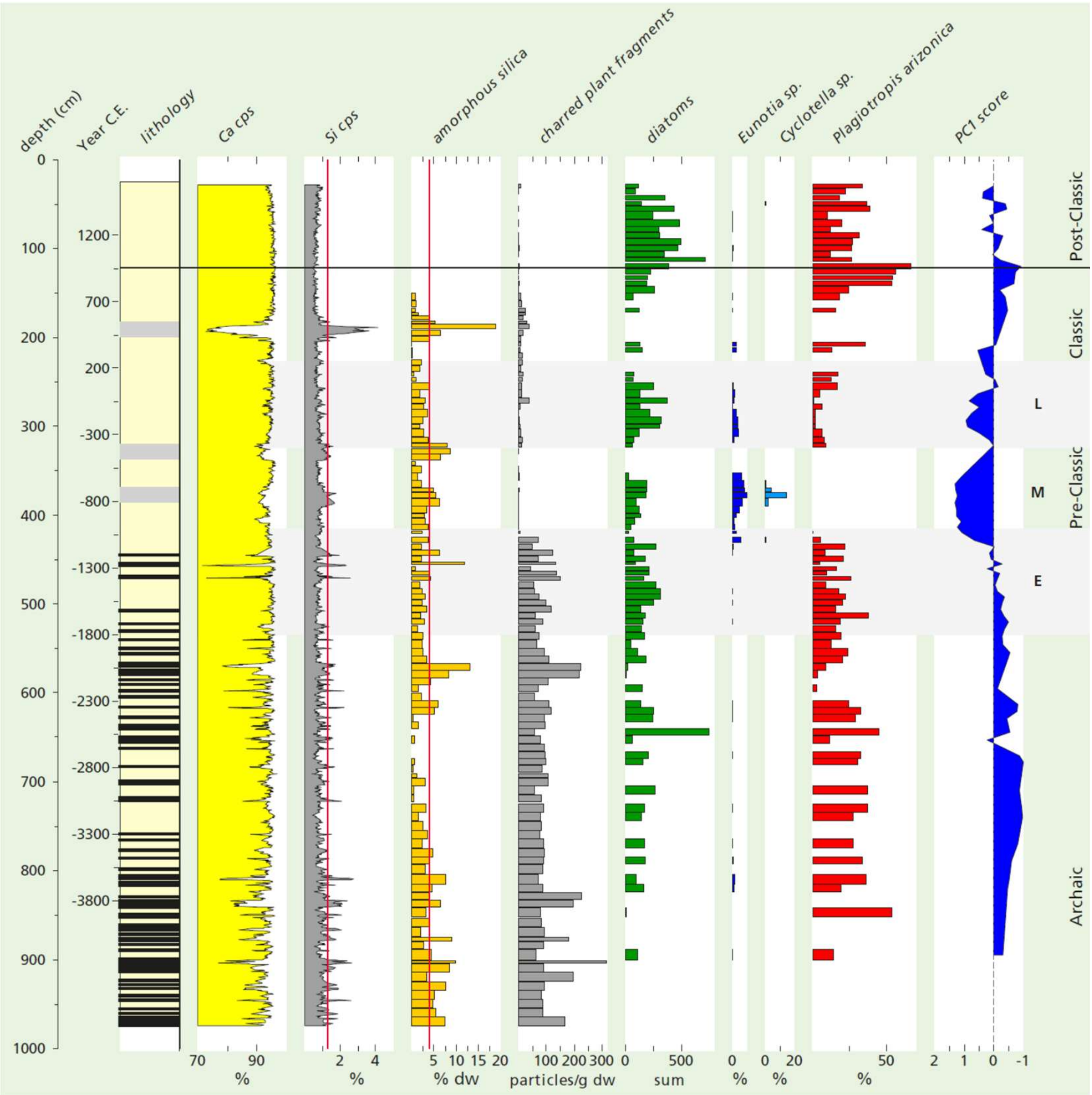

depth (cm)
Year C.E.
lithology
Ca cps
Si cps
amorphous silica
charred plant fragments
diatoms
Eunotia sp.
Cyclotella sp.
Plagiotropis arizonica
PC1 score
Post-Classic
Classic
Pre-Classic
Archaic
L
M
E
% dw
particles/g dw
sum
%

Fig. 3

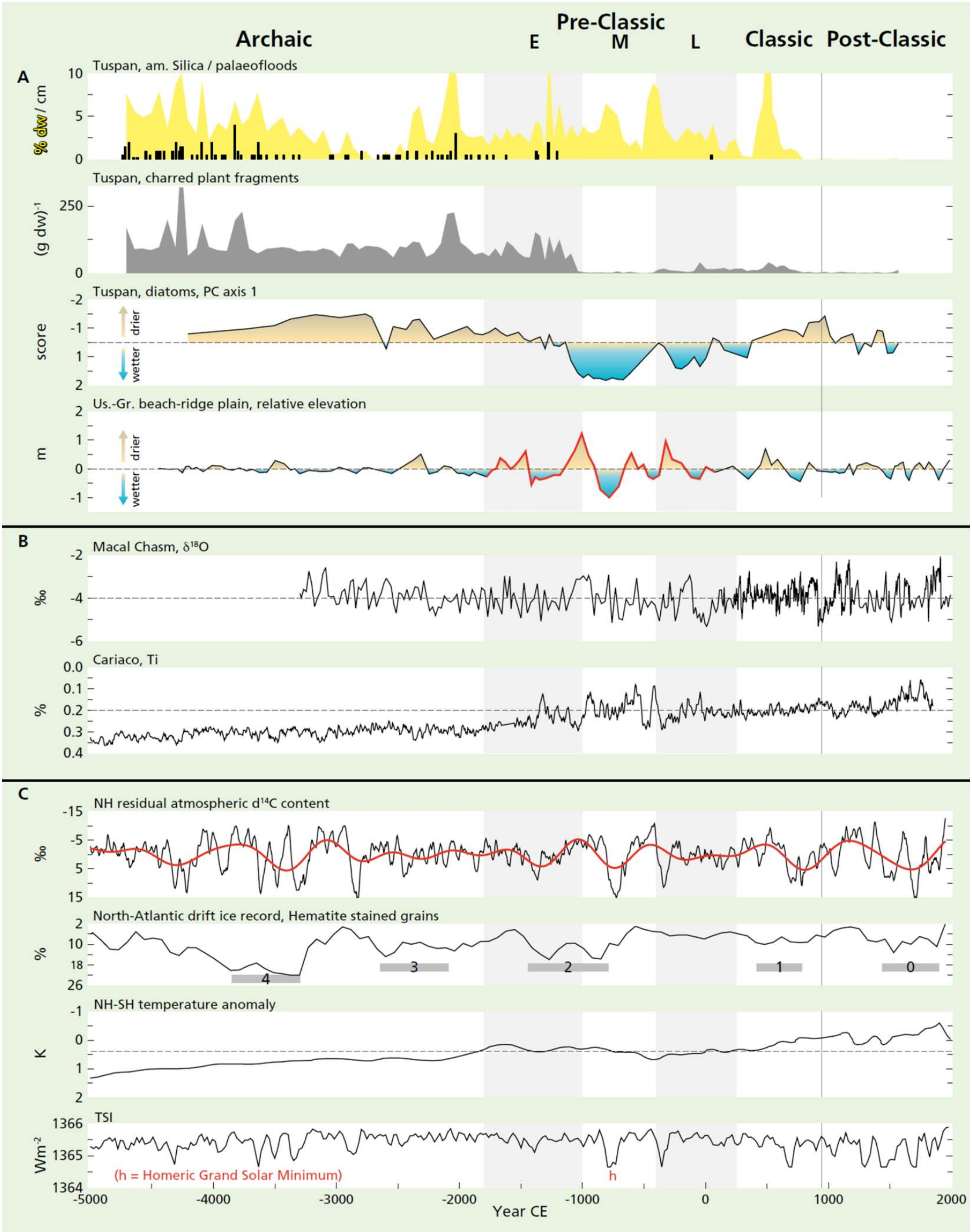

Archaic
Pre-Classic
E
M
L
Classic
Post-Classic
A
Tuspan, am. Silica / palaeofloods
% dw / cm
Tuspan, charred plant fragments
(g dw)-1
Tuspan, diatoms, PC axis 1
score
drier
wetter
Us.-Gr. beach-ridge plain, relative elevation
m
B
Macal Chasm, δ18O
‰
Cariaco, Ti
%
C
NH residual atmospheric d14C content
‰
North-Atlantic drift ice record, Hematite stained grains
%
4
3
2
1
0
NH-SH temperature anomaly
K
TSI
Wm-2
(h = Homeric Grand Solar Minimum)
h
Year CE

Fig. 4

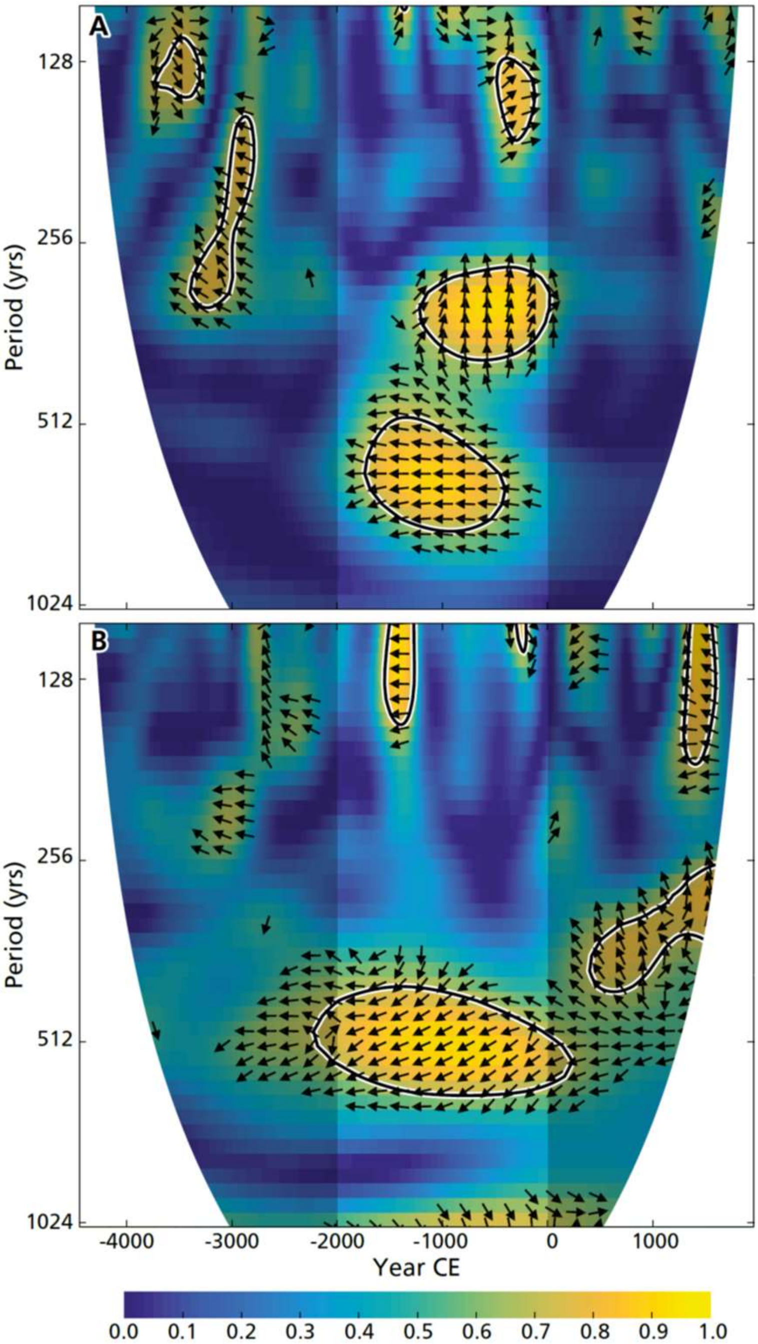
A
B
128
256
512
1024
Period (yrs)
-4000
-3000
-2000
-1000
0
1000
Year CE
0.0
0.1
0.2
0.3
0.4
0.5
0.6
0.7
0.8
0.9
1.0

Fig. 5

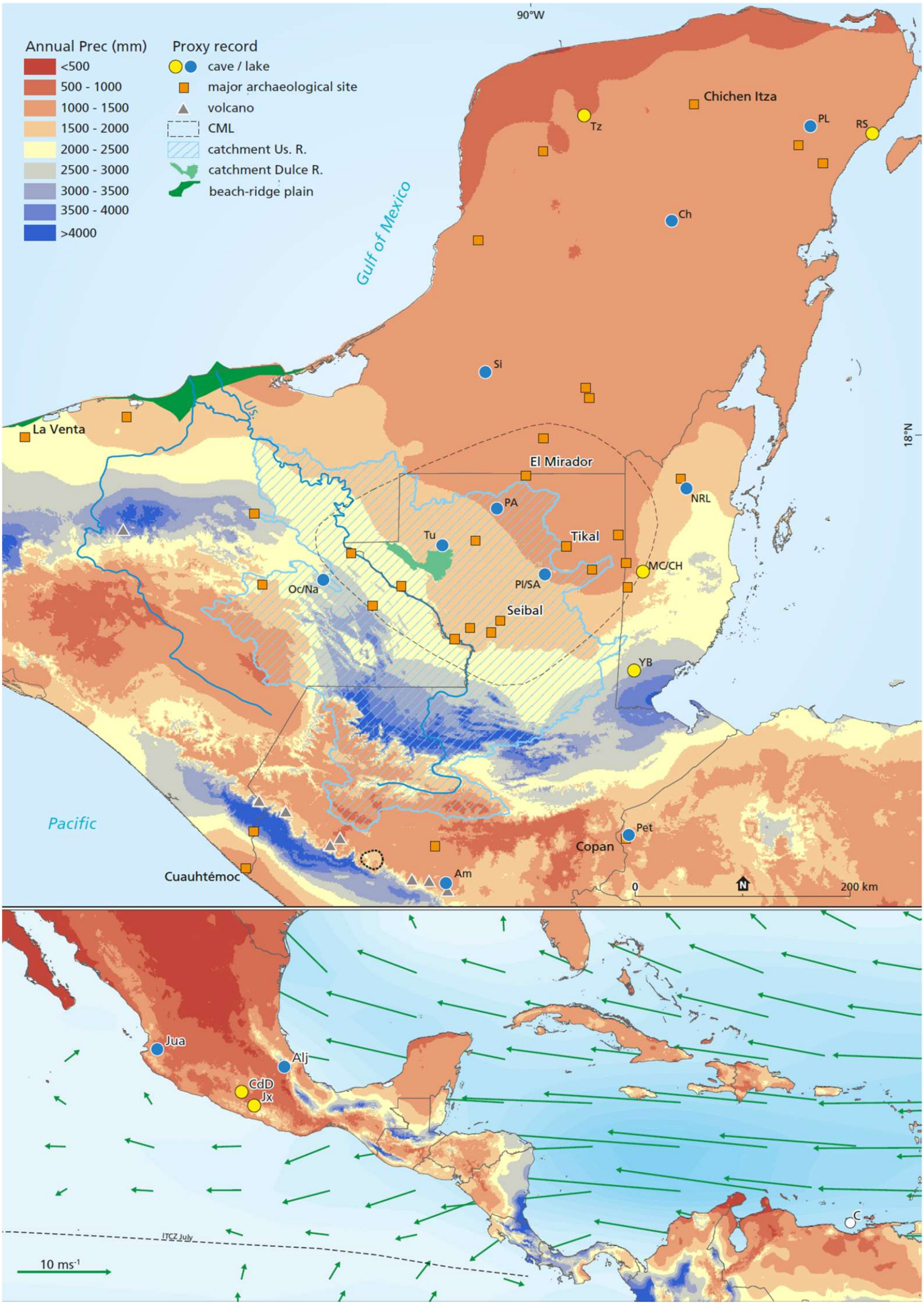

90°W
Annual Prec (mm)
<500
500 - 1000
1000 - 1500
1500 - 2000
2000 - 2500
2500 - 3000
3000 - 3500
3500 - 4000
>4000
Proxy record
cave / lake
major archaeological site
volcano
CML
catchment Us. R.
catchment Dulce R.
beach-ridge plain
Gulf of Mexico
Chichen Itza
Tz
PL
RS
Ch
Si
La Venta
El Mirador
PA
NRL
Tu
Tikal
MC/CH
Oc/Na
Pl/SA
Seibal
YB
18°N
Pacific
Pet
Copan
Cuauhtémoc
Am
0
200 km
Jua
Alj
CdD
Jx
C
ITCZ July
10 ms-1

Fig. A1

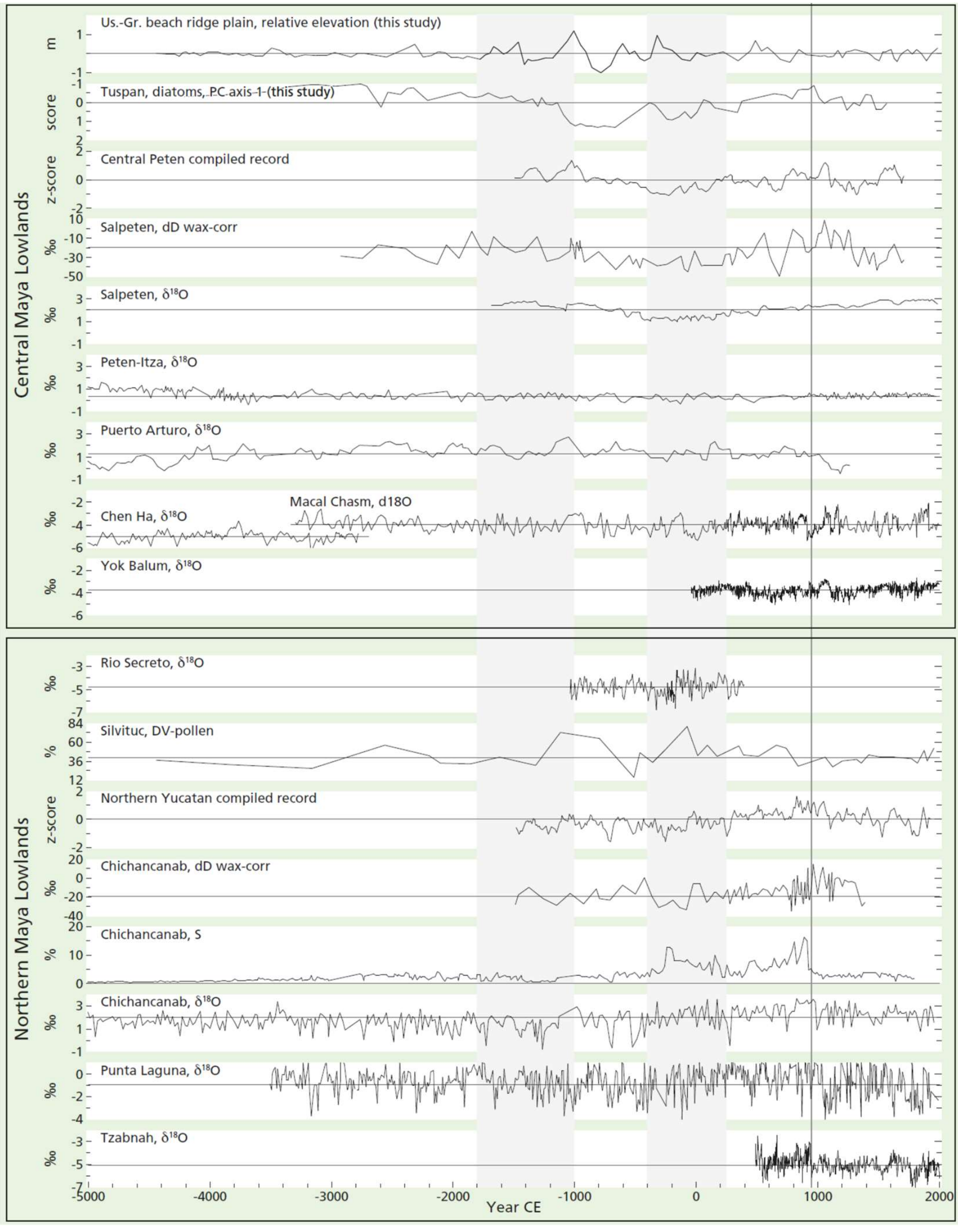

Central Maya Lowlands
Us.-Gr. beach ridge plain, relative elevation (this study)
Tuspan, diatoms, PC axis 1 (this study)
Central Peten compiled record
Salpeten, dD wax-corr
Salpeten, δ18O
Peten-Itza, δ18O
Puerto Arturo, δ18O
Macal Chasm, d18O
Chen Ha, δ18O
Yok Balum, δ18O
Northern Maya Lowlands
Rio Secreto, δ18O
Silvituc, DV-pollen
Northern Yucatan compiled record
Chichancanab, dD wax-corr
Chichancanab, S
Chichancanab, δ18O
Punta Laguna, δ18O
Tzabnah, δ18O
m
score
z-score
‰
%
Year CE
-5000
-4000
-3000
-2000
-1000
0
1000
2000

Fig. A2a

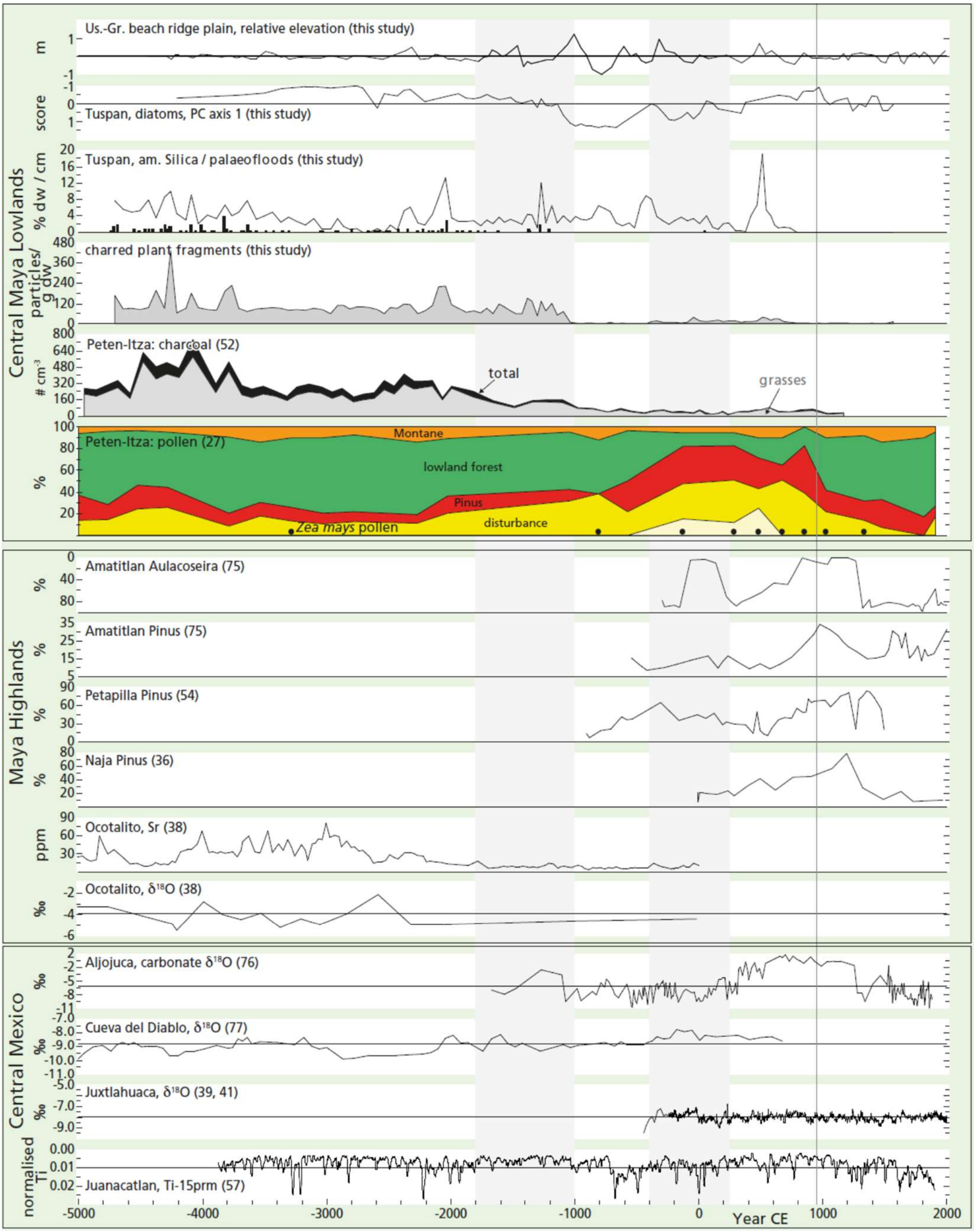

Central Maya Lowlands
Us.-Gr. beach ridge plain, relative elevation (this study)
m
score
Tuspan, diatoms, PC axis 1 (this study)
Tuspan, am. Silica / palaeofloods (this study)
% dw / cm
charred plant fragments (this study)
particles/ g dw
Peten-Itza: charcoal (52)
cm⁻³
total
grasses
Peten-Itza: pollen (27)
Montane
lowland forest
Pinus
disturbance
Zea mays pollen
%
Maya Highlands
Amatitlan Aulacoseira (75)
Amatitlan Pinus (75)
Petapilla Pinus (54)
Naja Pinus (36)
Ocotalito, Sr (38)
ppm
Ocotalito, δ18O (38)
‰
Central Mexico
Aljojuca, carbonate δ18O (76)
Cueva del Diablo, δ18O (77)
Juxtlahuaca, δ18O (39, 41)
normalised Ti
Juanacatlan, Ti-15prm (57)
Year CE
-5000
-4000
-3000
-2000
-1000
0
1000
2000

Fig. A2b

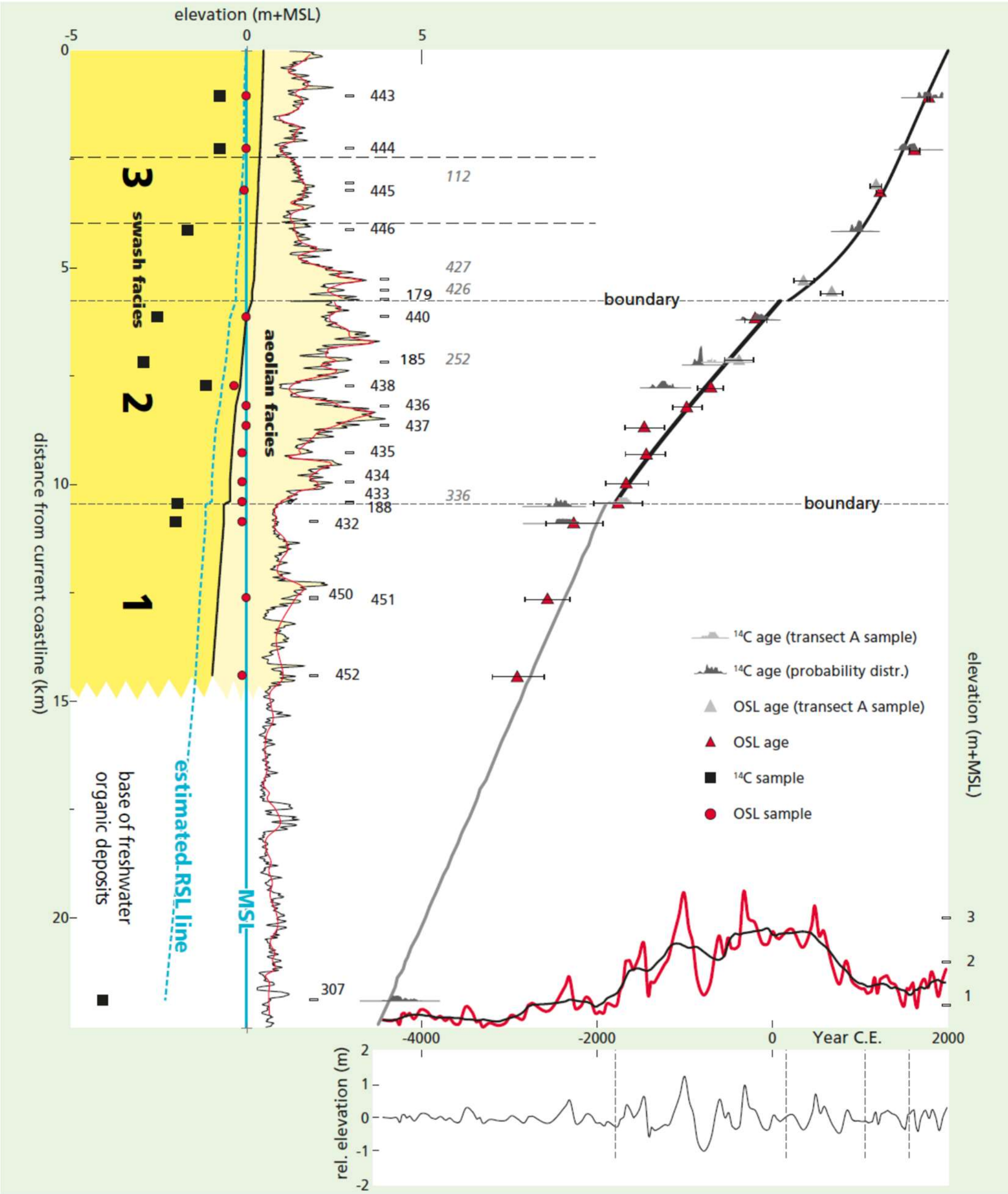
elevation (m+MSL)
distance from current coastline (km)
swash facies
aeolian facies
boundary
estimated RSL line
MSL
base of freshwater organic deposits
¹⁴C age (transect A sample)
¹⁴C age (probability distr.)
OSL age (transect A sample)
OSL age
¹⁴C sample
OSL sample
Year C.E.
rel. elevation (m)

Fig. A3

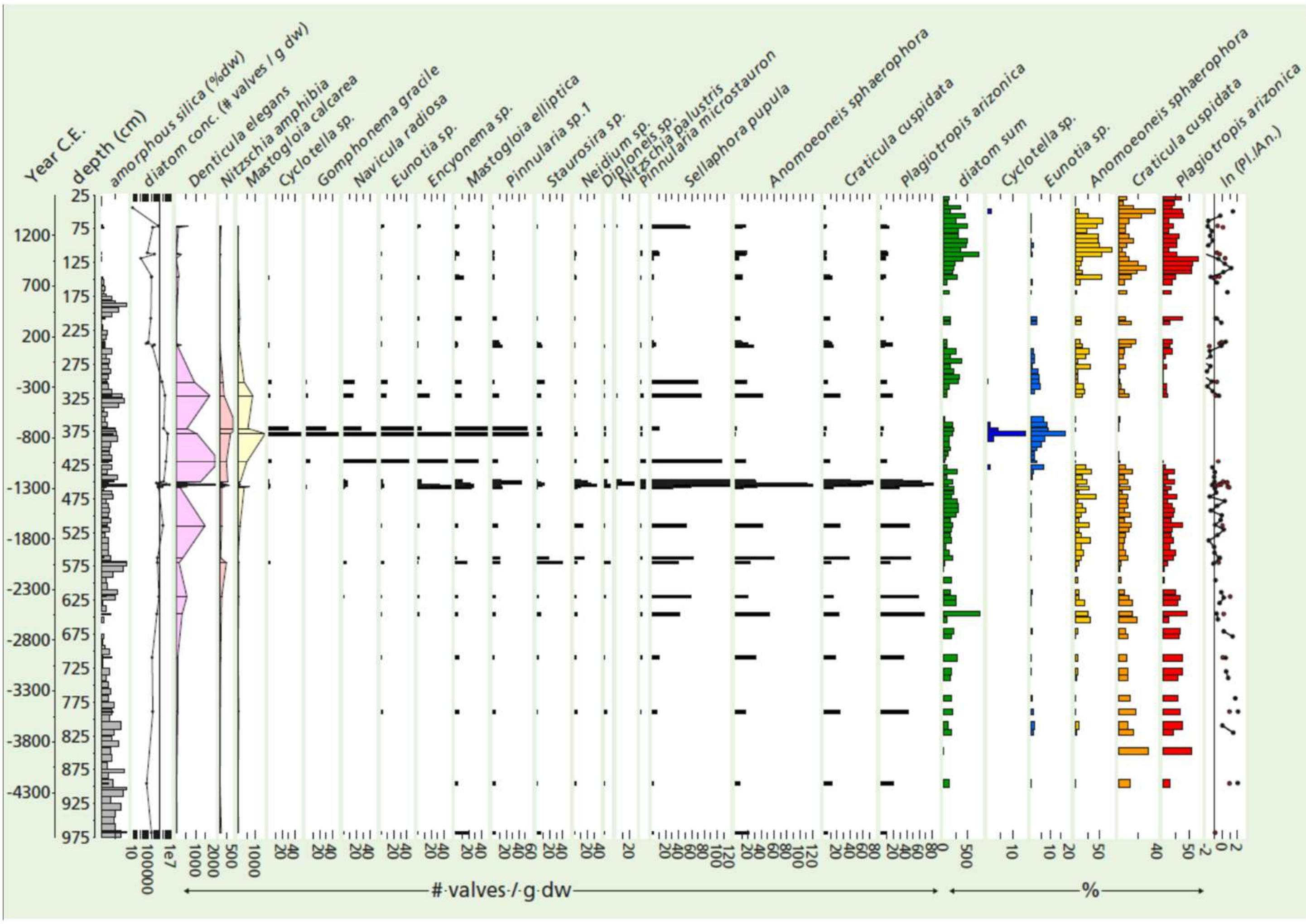

Fig. A4

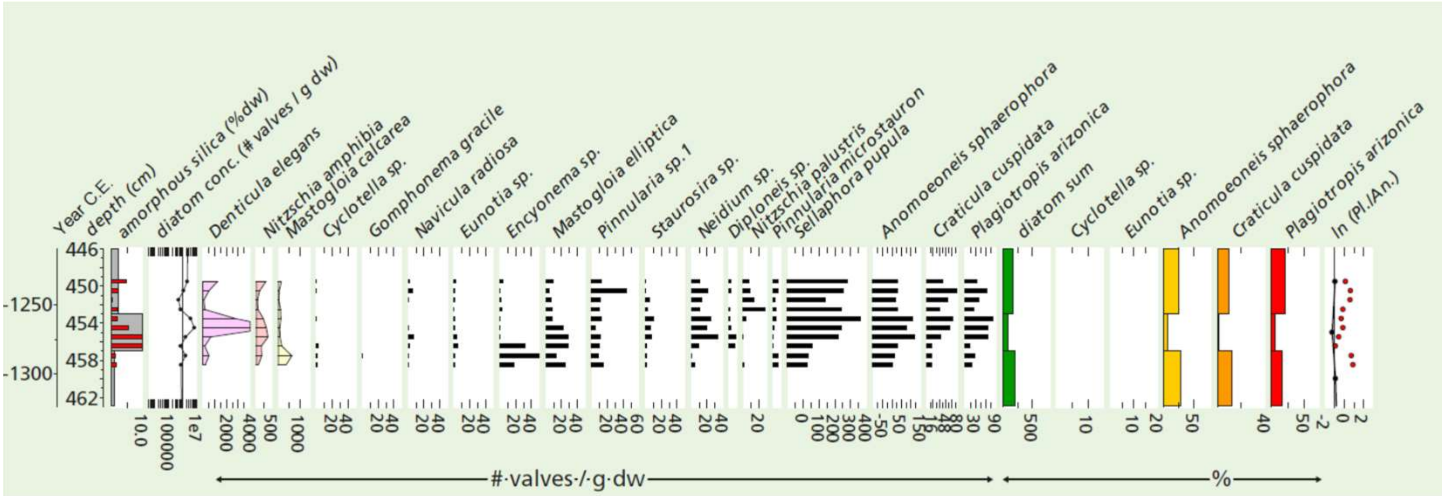

Fig. A5

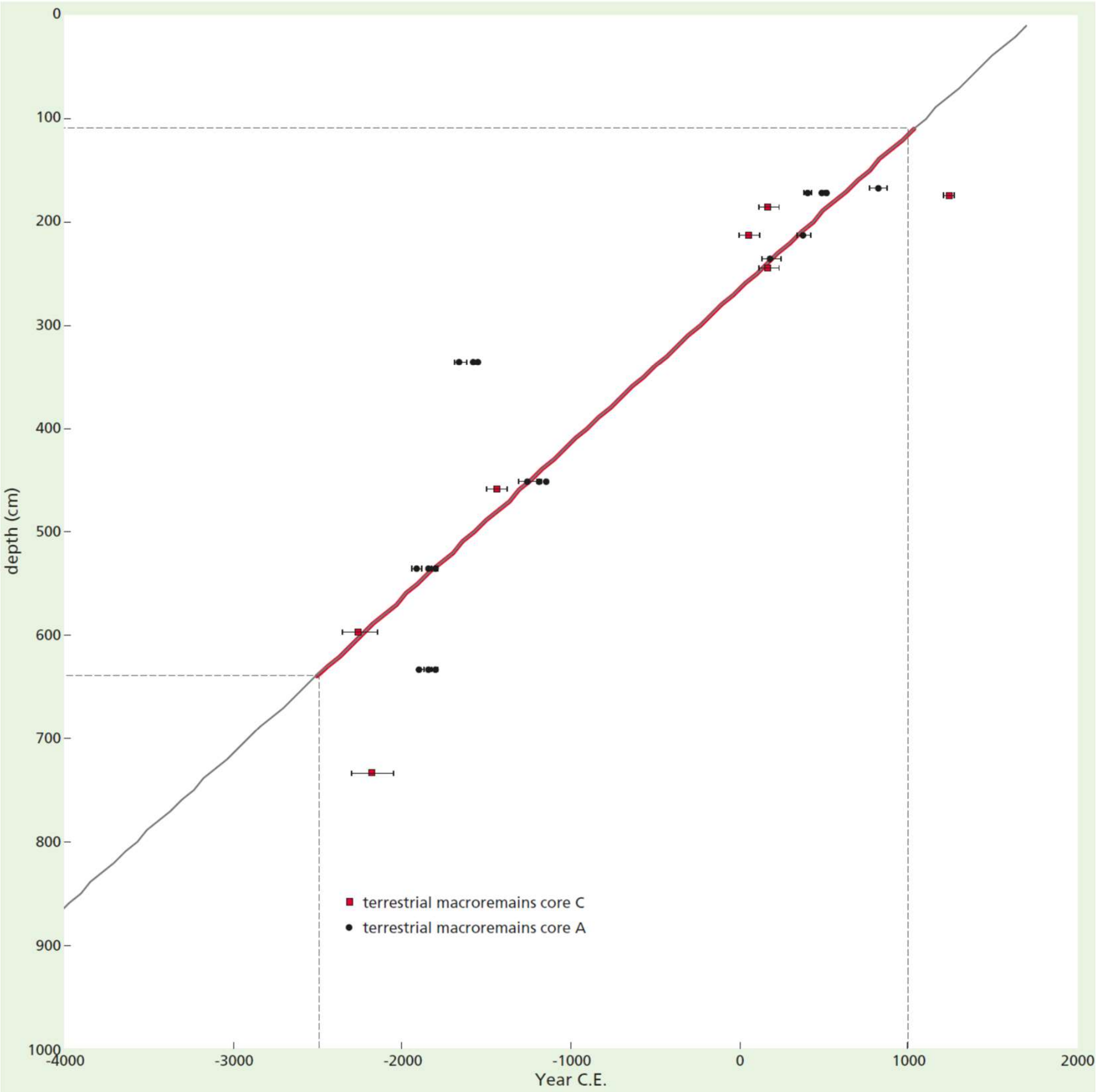

depth (cm)
Year C.E.
terrestrial macroremains core C
terrestrial macroremains core A
0
100
200
300
400
500
600
700
800
900
1000
-4000
-3000
-2000
-1000
0
1000
2000

Fig. A6

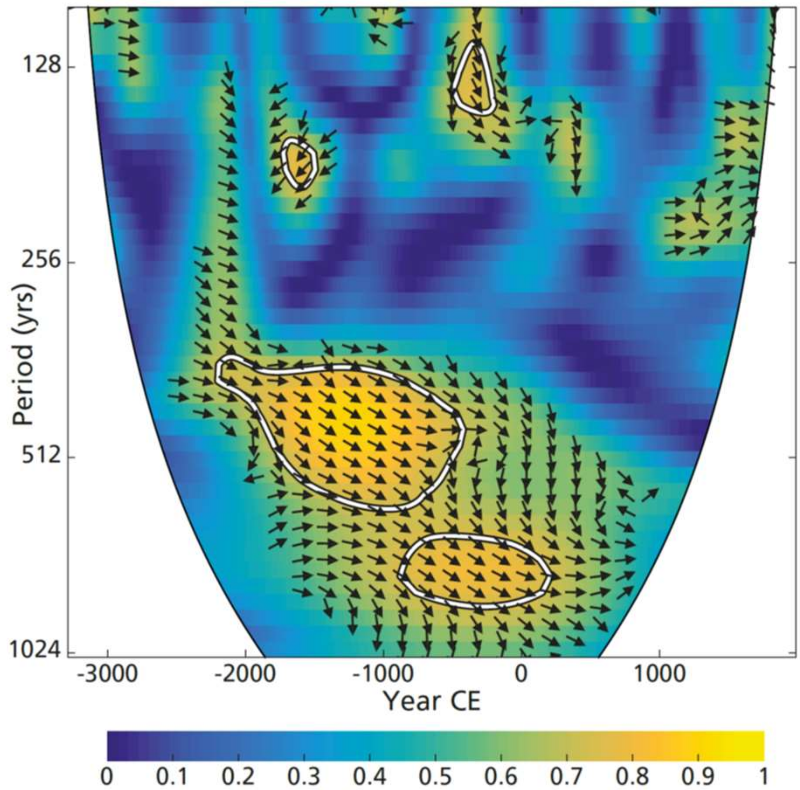
128
256
512
1024
Period (yrs)
-3000
-2000
-1000
0
1000
Year CE
0
0.1
0.2
0.3
0.4
0.5
0.6
0.7
0.8
0.9
1

Fig. A7

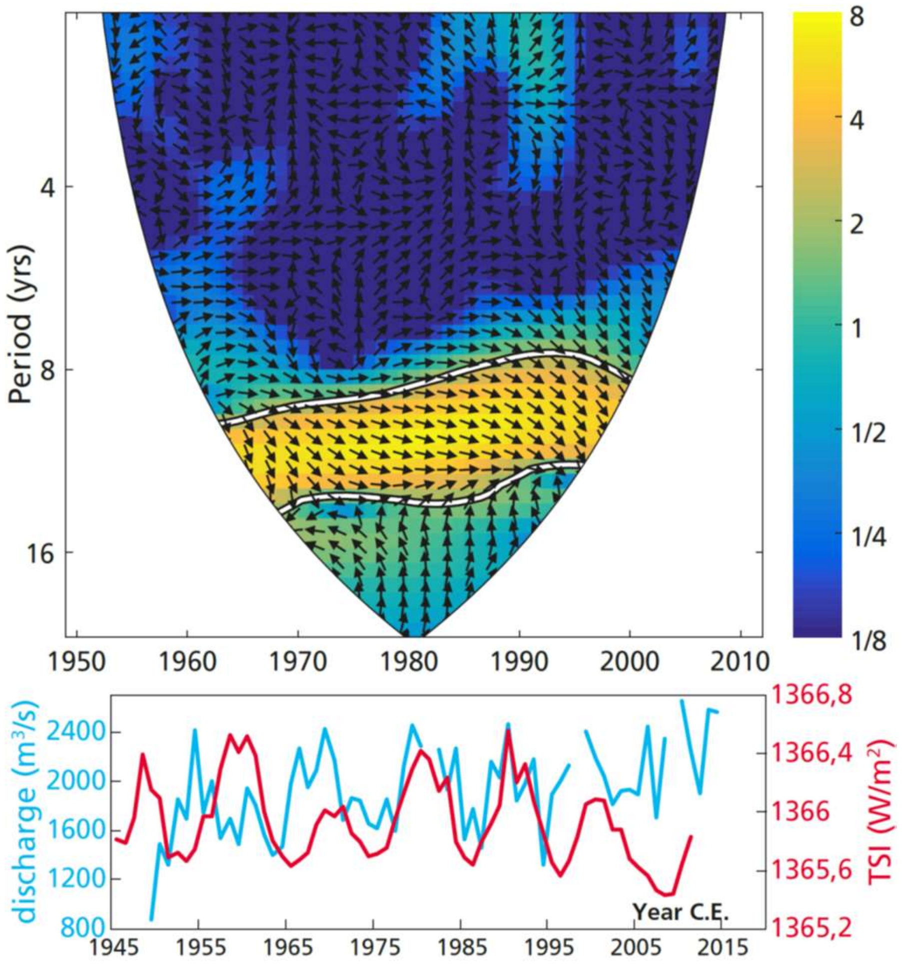
4
8
16
Period (yrs)
1950
1960
1970
1980
1990
2000
2010
8
4
2
1
1/2
1/4
1/8
discharge (m³/s)
2400
2000
1600
1200
800
1366,8
1366,4
1366
1365,6
1365,2
TSI (W/m²)
Year C.E.
1945
1955
1965
1975
1985
1995
2005
2015

Fig. A8

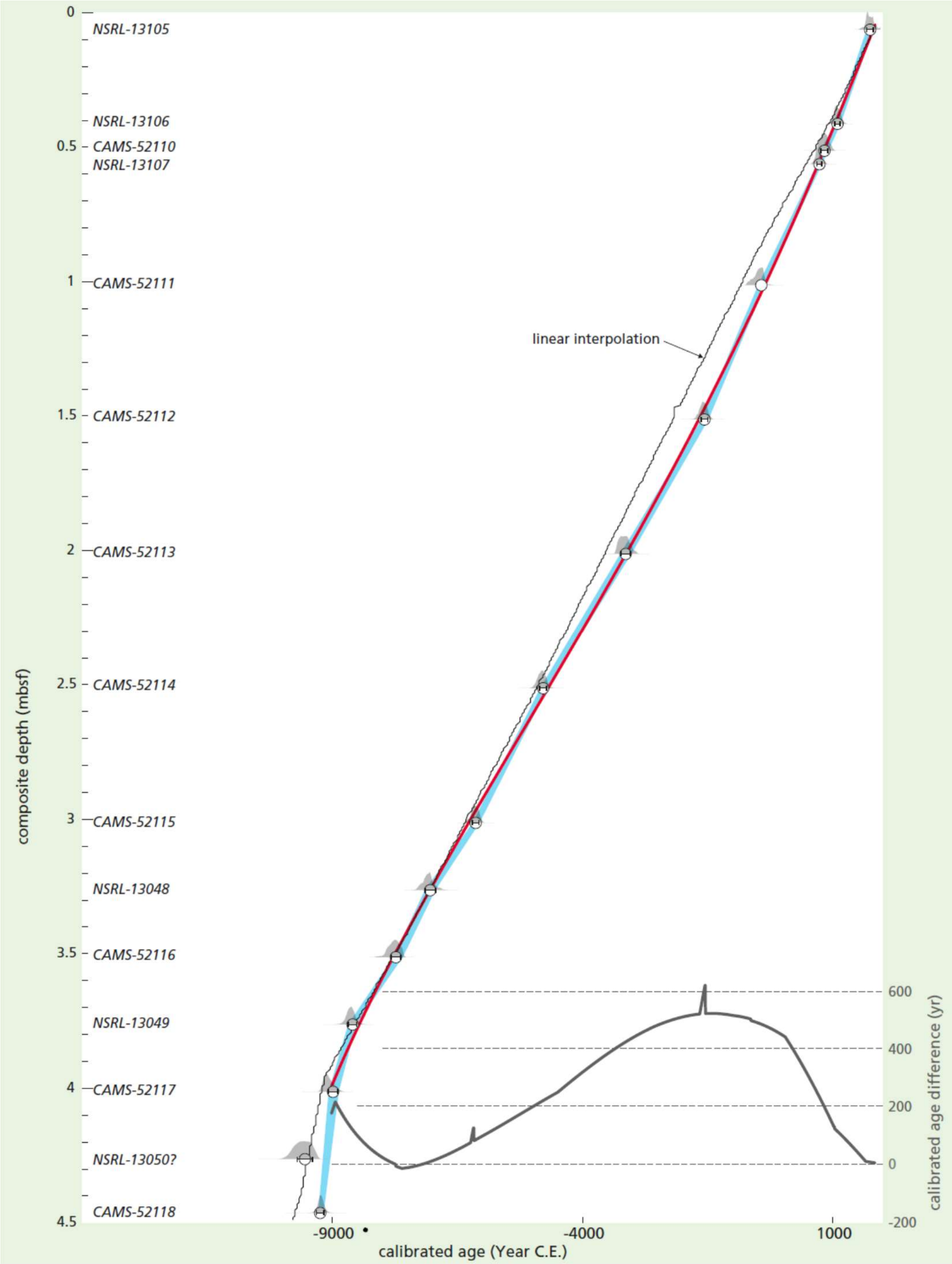
composite depth (mbsf)
calibrated age (Year C.E.)
calibrated age difference (yr)
linear interpolation
NSRL-13105
NSRL-13106
CAMS-52110
NSRL-13107
CAMS-52111
CAMS-52112
CAMS-52113
CAMS-52114
CAMS-52115
NSRL-13048
CAMS-52116
NSRL-13049
CAMS-52117
NSRL-13050?
CAMS-52118
0
0.5
1
1.5
2
2.5
3
3.5
4
4.5
-9000
-4000
1000
600
400
200
0
-200

Fig. A9